Research Article
DOI: http://dx.doi.org/10.2110/palo.2016.007
LATE CHATTIAN PLATFORM CARBONATES WITH BENTHIC FORAMINIFERA AND CORALLINE ALGAE FROM THE SE IBERIAN PLATE

TELM BOVER-ARNAL,[1] CARLES FERRÀNDEZ-CAÑADELL,[2] JULIO AGUIRRE,[3] MATEU ESTEBAN,[4, 5] JOSÉ FERNÁNDEZ-CARMONA,[5] EDUARD ALBERT-VILLANUEVA,[1] and RAMON SALAS[1]
[1]Departament de Geoquímica, Petrologia i Prospecció Geòlogica, Facultat de Geologia, Universitat de Barcelona. Martí i Franquès s/n, 08028 Barcelona, Spain
[2]Departament d'Estratigrafia, Paleontologia i Geociències Marines, Facultat de Geologia, Universitat de Barcelona. Martí i Franquès s/n, 08028 Barcelona, Spain
[3]Departamento de Estratigrafía y Paleontología, Facultad de Ciencias, Universidad de Granada. Fuentenueva s/n, 18002 Granada, Spain
[4]External Consultant, Repsol Exploración S.A. Méndez Álvaro 44, 28045 Madrid, Spain
[5]Szalai Grup S.L. Sant Jaume 11, 07314 Caimari (Selva), Mallorca, Spain
email: telm.boverarnalub.edu
ABSTRACT: The carbonate system studied represents an under-investigated sedimentary record formed in the western end of the Tethys during the Chattian relatively warm climate regime. These platform carbonates are examined with respect to rock fabrics, biostratigraphy, biostratinomy, paleoecology, and sequence stratigraphy. Dominant carbonate producers include scleractinian corals and echinoids, but the most prolific were symbiont-bearing benthic foraminifera and coralline algae. The presence of *Miogypsinoides complanatus* and *Miogypsinoides formosensis* indicates a late Chattian age (Shallow Benthic Zone 23). The depositional profile is consistent with a homoclinal ramp. The absence of a barrier margin and thus, of a lagoon, facilitated the transport and re-working of biogenic components throughout the platform. As a result, facies are rather homogeneous corresponding to a rudstone mainly formed by benthic foraminifera and coralline algae, which passes basinwards to deeper ramp to hemipelagic deposits rich in echinoids and planktonic foraminifera. Within this dominant facies, only subtle and gradual lateral variations on the relative abundance or absence of certain skeletal components or species are recognized, comprising two end members. A proximal biofacies of benthic foraminifera and coralline algae including corals in growth position, fragments of green algae, and seagrass dwellers where *Eulepidina*, *Nummulites*, and *Operculina* are absent, and a distal biofacies where corals, green algae, and seagrass dwellers are not present, but *Eulepidina*, *Nummulites* and *Operculina* are common. Carbonate deposition was controlled by long-term relative sea-level fluctuations including a Rupelian?–late Chattian transgression, a late Chattian regression, which ended in subaerial exposure of proximal ramp carbonates, and a latest Chattian to early Miocene transgression. The Chattian carbonate platform was finally drowned around the Oligocene/Miocene transition.
INTRODUCTION

The late Oligocene (Chattian) was characterized by a relative warm climate and reduced extent of Antarctic ice sheets between two major glaciations in the early Oligocene and the Oligocene/Miocene transition (Lear et al. 2000; Zachos et al. 2001; Alegret et al. 2008; Mudelsee et al. 2014). During this relatively warm period, carbonate platforms dominated by coralline algae and benthic foraminifera developed along the margins of the Tethys Sea (e.g., Buxton 1988; Schiavinotto and Verrubbi 1994; Fravega

et al. 1994; Parente 1994; Geel 1995; Kaiser et al. 2001; Knoerich and Mutti 2003; Bassi et al. 2007; Boukhary et al. 2008; Kuss and Boukhary 2008; Özcan et al. 2009, 2010; Brandano et al. 2009a, 2009b, 2010, 2012, 2015; Bassi and Nebelsick 2010; Işik and Hakyemez 2011; Reuter et al. 2013; Pomar et al. 2014; Brandano 2016), as well as in the Tethyan Seaway in the Iranian Plate (e.g., Elliott 1960; Berning et al. 2009; Reuter et al. 2009; Behforouzi and Safari 2011), and the Atlantic and Indo-Pacific realms (e.g., Wheeler 1963; Iturralde-Vinent ,1972; Cosico et al. 1989; Jurgan and Domingo 1989; Robinson 1995; Kumar and Saraswati 1997; Banerjee et al. 2000; Iryu et al. 2010; Madden and Wilson 2013). Some of these upper Oligocene deposits are of economic importance since they constitute hydrocarbon reservoirs in a number of areas, including onshore southwest Iran (Asmari Formation; Vaziri-Moghaddam et al. 2006; van Buchem et al. 2010; Sadeghi et al. 2011), Java Basin in Indonesia (Sharaf et al. 2005), offshore Palawan in the Philippines (Malampaya carbonate buildup; Fournier et al. 2004, 2005) and the Gulf of Venezuela (Perla Field; Pomar et al. 2015).

In the Tethyan realm, the Chattian carbonate platform systems have been mainly studied in its central and eastern parts. Studies reporting the occurrence and/or examining Chattian platform carbonates with coralline algae and benthic foraminifera from the western end of the Tethys are rare and mainly deal with Eocene and Rupelian strata (Geel 1995, 2000; Stoklosa and Simo 2008; Braga and Bassi 2011; Höntzsch et al. 2013). Moreover, the nature of most of the southeastern Iberian late Oligocene sedimentary record is continental (e.g., Jerez-Mir 1973, 1981; Geel 1996; Braga et al. 2002) or deep water (e.g., Geel 1995; Braga et al. 2002; Alegret et al. 2008; Fenero et al. 2013). Available data on Chattian platform carbonates from the southeastern Iberia mainly correspond to explanation notes of the Geological Map of Spain to a 1/50.000 scale of the Geological and Mining Institute of Spain (e.g., Vegas et al. 1973; Lendínez Gonzalez et al. 1993).

Under this context, the present paper documents Chattian platform carbonates of the Prebetic Domain (southeastern Iberian Peninsula) from sedimentological and paleontological standpoints. These rocks, formed in the western end of the Tethys Sea, correspond to an under-investigated sedimentary record of a phase of extensive carbonate platform development under relatively warm conditions, which should be taken into account in paleobiogeographic reconstructions of worldwide Chattian carbonate platform belts.

GEOLOGICAL SETTING

The Chattian rocks studied are located in the Prebetic Zone of the Betic Cordillera in the southeastern Iberian Peninsula (Fig. 1A). The Prebetic Domain, classically subdivided into the External Prebetic and Internal Prebetic units, is characterized by a suite of Mesozoic to early Cenozoic autochthonous deposits accumulated in the South Iberian passive continental margin (García-Hernández et al. 1980; Vera 2000; Braga et al. 2002). The External Prebetic corresponds to the northern part of the Prebetic Zone, located in a proximal position with respect to the southeastern Iberian paleomargin, and mainly comprises platform carbonates that were periodically interrupted by inputs of terrigenous sediments delivered from the adjacent emerged landmass. The Internal Prebetic is mainly formed by hemipelagic deposits including turbidites. It is located southwards of the External Prebetic, in a distal position with respect to the Iberian paleomargin, and corresponds to the basin counterpart of the coastal and platform settings characteristic of the External Prebetic (Martín-Chivelet and Chacón 2007; Höntzsch et al. 2013).

The outcrops studied belong to the Benitatxell Range, which is located to the east of the town of El Poble Nou de Benitatxell (SE Spain), in the eastern end of the

External Prebetic (Fig. 1A). The late Eocene–Oligocene was characterized in this area by regional uplift probably related to the Pyrenean collision (Azéma 1977; Roca 1992; Geel 1995). The late Chattian–Aquitanian time was marked by regional subsidence linked to the initial stages of the Betic foreland basin development or to the extensional opening of the València Trough (Fontboté et al. 1990; Roca 1992; Geel 1995). From the Aquitanian onward, the Prebetic basin underwent compression and tectonic inversion on account of the Betic orogeny, giving rise to the External Zones of the Betic Cordillera (Azéma 1977; Fontboté et al. 1990; Roca 1992; Geel 1995; Geel et al. 1998). The paleogeographic reconstruction of the Tethys during the late Oligocene (early Chattian, ~ 28 Ma) by Dercourt et al. (2000) places the Prebetic Domain around 31ºN latitude (Fig. 1B).

The stratigraphic record of the Benitatxell Range is characterized by a Cretaceous substrate (Fig. 2A), which is unconformably overlain by a Paleogene to Quaternary succession (Figs. 1A, 2B; Vegas et al. 1973; Lendínez Gonzalez et al. 1993). The overlying Paleogene succession is made up of Oligocene deposits, which exhibit a basal detritic unit (~ 14 m thick) topped by a 3-m thick conglomerate with carbonate clasts mainly of Paleocene age (Vegas et al. 1973). The limestone conglomerate passes upwards in the succession to nummulitic limestone (~ 110 m thick) including *Nummulites fichteli*, and this is followed by a sedimentary record around 200 m thick (Vegas et al. 1973), which includes echinoid-bearing limestone and a stratigraphic interval of interbedded marl and limestone (Fig. 2C) with globigerinids.

The uppermost part of the Oligocene record is characterized by a limestone interval up to ~ 40 m thick rich in lepidocyclinids. The present study is essentially engaged in the analysis of these lepidocyclinid limestones (Fig. 3A–3C), which also include abundant coralline algae and other benthic foraminifera, such as *Miogypsinoides*, *Neorotalia*, *Risananeiza*, *Nummulites*, *Operculina*, *Heterostegina*, *Spiroclypeus*, *Cycloclypeus*, *Amphistegina*, and *Victoriella*.

Small patches of late Oligocene platform carbonates up to 9 m thick (Fig. 3D) rich in coralline algae, benthic foraminifera, and scleractinian corals outcropping in the Rebaldí area, 3.5 km north of Benitatxell Range, were also examined (Fig. 1A). This northern disseminated sedimentary record unconformably overlies Cretaceous well-bedded wackestone limestone (Fig. 3E) with planktonic foraminifera, and locally shows an up to 1-m thick basal conglomerate lag.

The early Miocene is mainly distinguished by a hundreds-of-meters thick succession of marl (Fig. 3F) and silty to sandy limestone containing abundant planktonic foraminifera, mainly globigerinids, and glauconite. Locally, unconformable conglomerate deposits attributed to the late Miocene occur (Fig. 1A). The Quaternary sediments and rocks mainly correspond to gray and red clay, calcareous breccia and to beach, dune and marsh deposits (Vegas et al. 1973).

MATERIALS AND METHODS

Three stratigraphic sections were logged in up to kilometric spaced sectors exhibiting the best exposure conditions found along the Chattian carbonates cropping out in the Benitatxell Range (Figs. 1A, 2A, 2B, 4, 5), from northeast to southwest: (1) Torre Garcia-Cim del Sol Road section (135 m thick); (2) Accés Sud Road section (27 m thick); and (3) Albacete Road section (32 m thick). An additional stratigraphic log, Rebaldí section (13 m thick), is presented for the Chattian disseminated platform carbonates located to the north of the Benitatxell Range (Figs. 1A, 3D, 3E, 6). Sedimentological, stratigraphical and paleontological field observations were complemented with a petrographic analysis of 134 thin sections with surface areas of 28 mm × 48 mm, 48 mm × 56 mm, and 56 mm × 78 mm. The Chattian limestones with

benthic foraminifera and coralline algae examined commonly lack clear bedding planes (i.e., Fig. 3B, 3C), and the sedimentary structures recognized are restricted to scarce bioturbation structures. Moreover, only minor facies differences including variations in the relative proportion (or absence) of the distinct fossil biota identified and local changes in the rock texture were observed (Figs. 4–6). Therefore, distinct lithofacies assemblages were not distinguished within this Chattian record. In addition, to place the benthic foraminifera- and coralline algae-bearing strata into a sequence-stratigraphic framework and to better understand their geological context, the lithostratigraphic units overlying and underlying these Chattian rocks were analyzed at the Torre Garcia-Cim del Sol Road section (Fig. 4). The contact between the Cretaceous substrate and the examined Oligocene rocks was investigated in the Rebaldí section (Figs. 1A, 3E, 6).

Taxonomic identification of benthic foraminifera and coralline algae was performed on randomly oriented sections. Samples of marls were washed, dried and sieved to obtain loose specimens of planktonic and benthic foraminifera for microfossil content and taxonomic determinations. Carbonate textures follow the classification schemes of Dunham (1962) and Embry and Klovan (1971). This paper uses 'early' and 'late' to qualify both time-rock units and geologic time units following Zalasiewicz et al. (2004).

Biotic components, quartz, and glauconite were qualified by using three categories: (1) Facies-characteristic component; (2) common component; and (3) rare component (Figs. 4–6). The abundance of the different coralline algal taxa identified was quantified in the Benitatxell Range by point counting (2100-point net). Qualitative evaluation of test degradation on benthic foraminifera follows the numerical scale by Beavington-Penney (2004): (0) *in situ*; (1) moderate transport/wave re-working; (2) extensive transport/wave re-working; and (3) may reflect transport distance much greater than in category 2, or transport within turbidity currents, or predation by large bioeroders such as fish and echinoids. On other biogenic components, as well as at the scale of microfacies, the qualitative estimation of pre-burial taphonomic features including abrasion, fragmentation, bioerosion and encrustation, used two categories: (1) low and (2) high (Figs. 4–6).

A transgressive-regressive (T-R) sequence-stratigraphic analysis (see Catuneanu et al. 2011) was carried out to interpret the changes in accommodation during deposition of the carbonate successions studied. The reduced extent and bad exposure conditions of the outcrops (e.g., Fig. 3B, 3C) did not always permit recognizing stratal terminations or stacking patterns, and thus, to perform a three- or four-systems tract-based sequence-stratigraphic analysis (i.e., Catuneanu et al. 2011). Therefore, the T-R sequence-stratigraphic analysis applied to these carbonate successions is based on the identification of surfaces that mark large-scale changes in facies trend from deepening- to shallowing-upwards, or vice versa. The surfaces with sequence-stratigraphic significance used in the study correspond to a maximum flooding surface and sequence boundaries, which include subaerial unconformities and a maximum regressive surface.

CHARACTERIZATION OF THE CHATTIAN CARBONATES FROM THE BENITATXELL RANGE

The coralline algal limestones with lepidocyclinids examined are essentially dark gray massive rudstone (Figs. 4, 5, 7A). The intergranular space in these grain-dominated fabrics is mainly filled with micrite (Fig. 7B). However, rudstone beds with calcite cement filling the intergranular space are locally present. Primary aragonitic skeletons of green algae and corals are replaced by calcite. Fractures, as well as primary intraskeletal porosity of coralline algae and benthic foraminifera, are also commonly occluded by sparry calcite. Stylolites are frequent along the rims of lepidocyclinid tests.

Packstone to floatstone textures are uncommon (Figs. 4, 5). Non-skeletal components identified correspond to peloids and silt- to sand-sized quartz particles, which occur locally with abundances ranging from rare to common (Figs. 4, 5). Quartz grains do not surpass abundances of 1%. Glauconite occurs as a rare component in the Torre Garcia-Cim del Sol Road section from meter 114 to meter 124 (Fig. 4).

Fossil Assemblages

Skeletal components in the Chattian limestones are dominated by benthic foraminifera and coralline algae. A detailed account of these fossil assemblages is provided below. Other identified biotic components correspond to fragments and entirely-preserved specimens of mollusks (Fig. 7C), green algae, echinoids, bryozoans, scleractinian corals, microbialites, *Ditrupa* sp., other worm tubes, and planktonic foraminifera. The colonial corals found in life position exhibit sheet-like, platy, massive and domal morphologies, and occur isolated giving rise to an unbound growth fabric. The stratigraphic distributions and qualitative abundances of the main biota recognized in these Chattian limestones are shown in figures 4 and 5.

Coralline Algae.—Coralline algae occur mainly as fragments of crusts or branches scattered among benthic foraminifer tests or forming rhodoliths (Figs. 4, 5, 7D). Limestones are well cemented, thus precluding the extraction of isolated rhodoliths. Therefore, we could not perform a shape analysis of the rhodoliths following the methodology of Bosence (1976, 1983). However, different sections in the outcrop indicate that they are ellipsoidal-spheroidal in shape (Fig. 7D).

Rhodoliths are nucleated. Nuclei are made up of benthic foraminifers, or fragments of calcareous algae, bryozoans, balanids, echinoids, and corals. More rarely, nuclei are fragments of lithified sediment. The rhodoliths are made up of complex intergrowth of different species of coralline algae, the main contributor to the rhodolith formation, with bryozoans, serpulid tubes, and encrusting benthic foraminifers. Locally, molds of vermetid gastropods are also present. Predominant coralline algal growth forms are warty and fruticose. Encrusting and laminar growth forms are less common.

Up to ten species of non-geniculate corallines belonging to six genera have been identified: *Lithothamnion ramosissimum* (Fig. 8A), *Lithothamnion peleense*, *Lithothamnion* sp. 1, *Lithothamnion* sp. 2, *Mesophyllum* sp. 1 (Fig. 8B), *Sporolithon lugeonii* (Fig. 8C), *Spongites* sp. 1 (Fig. 8D), *Spongites* sp. 2 (Fig. 8E), *Neogoniolithon contii* (Fig. 8F), and *Aethesolithon* sp. Together with the identified species, an unidentified laminar algal species is observed. The thallus shows a dorsiventral dimerous organization, with primigenous filaments made up of palisade cells. The postigenous filaments consist of one to two rows of cells, increasing the thickness surrounding conceptacles. Cell fusions are conspicuous. One sporangial conceptacle is observed, but unfortunately the numbers of porous on the roof is not visible, precluding a precise generic assignment. In addition to non-geniculate corallines, a few calcified portions of geniculate ones are also seen. Their taxonomic identification is not possible since neither enough vegetative traits nor reproductive structures have been preserved. However, they show cell fusions, so that attribution to the genus *Amphiroa* can be excluded.

In terms of abundance, members of the order Hapalidiales (~ 75% of the total assemblages) are dominant, followed by Sporolithales (~ 17%), and Corallinales (~ 8%). The most abundant species are *Lithothamnion ramosissimum* and *Mesophyllum* sp., followed by *Sporolithon lugeonii*. *Aethesolithon* sp. and geniculate corallines are very rare (less than 1% all together).

Benthic Foraminifera.—Identified benthic foraminifera include *Miogypsinoides formosensis* (Fig. 9A), *Eulepidina dilatata* (Fig. 9B), *Eulepidina elephantina* (Fig. 9C;

specimen sizes of up to 5 cm diameter), *Eulepidina raulini*, *Nephrolepidina* sp., *Nummulites* cf. *vascus*, *Nummulites* cf. *bouillei*, *Operculina complanata*, *Heterostegina assilinoides* (Fig. 9D), *Spiroclypeus blanckenhorni* (Fig. 9E), *Cycloclypeus* aff. *mediterraneus*, *Risananeiza pustulosa* (Fig. 9F), *Neorotalia viennotti* (Fig. 9G), *Amphistegina bohdanowiczi*, *Amphistegina mammilla*, *Victoriella conoidea*, *Austrotrillina asmariensis*, other miliolids, *Peneroplis* sp., *Sphaerogypsina* sp., *Gypsina vesicularis*, *Planorbulina* sp., *Planorbulinella* sp., *Carpenteria* sp., *Lenticulina* sp., *Nodosaria* sp., and textularids. Their stratigraphic distributions and qualitative abundances are shown in figures 4 and 5.

Biostratinomy

Microtaphofacies were analyzed on coralline algae, symbiont-bearing benthic foraminifera and other minor constituents to determine how these skeletal components accumulated, were altered, and differentially preserved in the rock record of the Benitatxell Range. Biogenic components are generally well preserved but commonly show pre-burial taphonomic alteration by encrustation, fragmentation, abrasion, and bioerosion. Some relevant studies on this subject include Nebelsick and Bassi (2000), Checconi and Monaco (2008), Nebelsick et al. (2011), Silvestri et al. (2011), Ćosović et al. (2012) and Nitsch et al. (2015).

Encrustations are present in many of the thin sections studied (Figs. 4, 5). Encrustation is mainly performed by coralline algae. However, bryozoans, serpulids and foraminifera, such as *Gypsina* and *Planorbulina,* are also common encrusters. Complex multi-taxon encrustation sequences occur (i.e., rhodoliths; Fig. 10A). Encrustation sequences are commonly affected by other taphonomic processes, such as bioerosion.

Bioerosion is generally low (Figs. 4, 5), although it can be locally high on *Eulepidina elephantina* tests and rhodoliths (i.e., from meter 85 to meter 95 in the Torre Garcia-Cim del Sol Road section and around meter 3 in the Accés Sud Road section; Figs. 4, 5). Cement- and/or sediment-filled rounded holes mainly produced by lithophagid bivalves (*Gastrochaenolites* sp.) are easily recognizable on coral skeletons and rhodoliths. Sack-like borings with a narrow aperture channel that ends in an ellipsoidal or irregular wider chamber, *Trypanites*-like borings and other nonspecific boring structures are as well discernible on large lepidocyclinids (Fig. 10B), rhodoliths, corals, and other skeletal components. The sack-like bioerosional structures are connected in places. Locally, bioerosion by sponges (i.e., *Entobia*) occurs on coralline algae crusts and rhodoliths.

Fragmentation of skeletal components is mostly high in the microfacies analyzed (Figs. 4, 5), and mainly affects coral colonies, lepidocyclinids, thin coralline algal thalli, bivalves, gastropods, green algae, and echinoids (Fig. 10C). Size of skeletal fragments is very variable and commonly ranges between > 1 mm and < 4 cm. However, fragments of lepidocyclinids, corals, and rhodoliths > 4 cm do occur.

Abrasion features caused by grain agitation during transport and biological activity were mainly observed in high abundances (Figs. 4, 5) on benthic foraminifera and rhodoliths. Rhodoliths commonly exhibit low abrasion of their external coralline thalli. However, undamaged rhodoliths occur as well. Undamaged tests of symbiont-bearing benthic foraminifera are very scarce. Test degradation features on benthic foraminifera mainly range from shallow pits, which do not penetrate the outer wall, to disintegration of the entire test thickness (Fig. 10D). These observations would include 1 to 3 categories on the scale of taphonomic features observed in fossil *Nummulites* by Beavington-Penney (2004).

CHARACTERIZATION OF THE CHATTIAN CARBONATES FROM THE REBALDÍ OUTCROPS

The carbonates studied mainly consist of decimeter- to meter-thick rudstone beds. Micrite commonly fills in spaces between grains. Locally, packstone (Fig. 11A), grainstone, and framestone textures occur. The limestones are light- to dark-gray in color (Fig. 3D). Sparry calcite is present replacing primary aragonitic skeletons of green algae and scleractinians, and in places in intraskeletal pore spaces of biogenic components, as well as occluding secondary porosity in the micrite matrix and filling fractures. Peloids are common non-skeletal constituents of the facies, whereas silt- to sand-sized quartz grains are rare (Fig. 6). Prograding clinoforms are exposed in the outcrop (Fig. 3D).

Fossil Assemblages

Colonial corals, benthic foraminifera, and coralline algae are dominant biogenic components in the limestones investigated in the Rebaldí outcrops. Detailed descriptions and inventory of benthic foraminifera and coralline algae identified are provided in the following sections. Corals occur as both fragments and wholly preserved specimens. The latter are found in growth position and show branching (Fig. 11B), platy, sheet-like, domal and massive morphologies. Scleractinians mainly exhibit a loose and unbound growth fabric. However, metric coral framestones ('patch reefs') made up of platy and sheet-like colonies give rise to platestone and sheetstone locally (*sensu* Insalaco 1998).

Subordinate skeletal components recognized include fragments, as well as entirely preserved fossils of mollusks, green algae (Fig. 11C), echinoids, bryozoans, *Ditrupa* sp., other serpulids, and planktonic foraminifera. The top of the carbonate succession is characterized by the occurrence of pervasive *Paronipora* (=*Microcodium*) structures (Figs. 3D, 11D). The qualitative occurrences of the fossil assemblages recognized in the Rebaldí section are detailed in Figure 6.

Coralline Algae.—In the Rebaldí section, coralline algae occur as abraded fragments. Relative abundance of coralline algae ranges from 5% to 10%. The great majority of fragments are foliose encrusting thalli; very rarely fragments of branches can be seen. Due to fragmentation and abrasion, most of the algal portions lack enough vegetative and reproductive characters to be reliably identified. Therefore, classification even at higher taxonomic level is precluded. This impedes, in turn, to estimate the relative abundance of taxa.

Among the identifiable algal fragments, six species can be recognized: *Sporolithon* sp. (Fig. 12A), *Lithothamnion* sp. 1 (Fig. 12B), *Lithothamnion* sp. 3 (Fig. 12C), *Mesophyllum* sp. 2 (Fig. 12D), *Spongites* sp. 1, and a laminar algal showing dorsiventral dimerous organization (Fig. 12E) as the one described in the Benitatxell Range. In addition, calcified portions of geniculate algae are also present. One of these algae is articulated, showing two calcified intergenicula articulated by non- or poorly calcified genicula (Fig. 12F). Further to corallines, the peyssonneliacean *Polystrata alba* is also present (Fig. 12G), but was only identified in one thin section (meter 10; Fig. 6).

Benthic Foraminifera.—The taxonomic study yielded *Planorbulina* sp. (Fig. 13A), *Planorbulinella* sp. (Fig. 13B), *Peneroplis thomasi* (Fig. 13C), *Schlumbergerina alveoliniformis*, *Praebullalveolina* aff. *oligocenica*, cibicidids, *Austrotrillina asmariensis* (Fig. 13D), other miliolids, *Nephrolepidina* sp., *Amphistegina bohdanowiczi* (Fig. 13E), *Neorotalia viennoti*, *Neorotalia lithothamnica* (Fig. 13F), *Miogypsinoides complanatus* (Fig. 13G), *Sphaerogypsina* sp. (Fig. 13H), gypsinids, *Spiroclypeus blanckenhorni* (Fig. 13I), *Risananeiza pustulosa* (Fig. 13J), *Heterostegina* aff. *assilinoides* (Fig. 13K), *Cycloclypeus* aff. *mediterraneus*, *Miniacina* sp., *Carpenteria* sp. (Fig. 13L), *Solenomeris* sp., *Haddonia heissigi* (Fig. 13M), *Nodosaria*

sp., and textularids. The stratigraphic distribution and qualitative abundance of these benthic foraminifera are detailed in Figure 6.

Biostratinomy

Pre-burial taphonomic signatures in the microfacies from the Rebaldí section mainly include abrasion, fragmentation, encrustation, and bioerosion. The biostratinomic patterns are similar to those described above for the samples from the Benitatxell Range (Fig. 10). Fragmented and abraded biogenic components occur in high abundances (Figs. 6, 11A), though well-preserved fossil coral skeletons and benthic foraminifera tests are common. Fragmentation particularly affects green algae, corals, mollusks, coralline algal thalli, and benthic foraminifera (Fig. 11A). Size of skeletal fragments mainly varies between > 1 mm and < 2 cm. Nevertheless, fragments of coralline algal branches and corals are usually > 2 cm. Test degradation on symbiont-bearing benthic foraminifera principally includes categories 2 and 3 on the scale of taphonomic features by Beavington-Penney (2004).

Presence of borings is low in the samples (Fig. 6). It is represented by *Gastrochaenolites* occurring in coral skeletons, borings produced by clionid sponges (*Entobia*) in corals and algal fragments, and by *Trypanites*-like borings recognized in fragments of mollusks. Encrustation is high (Fig. 6), and mostly due to coralline algae around fragments of corals. Encrustation sequences are commonly multigeneric including different genera of coralline algae, bryozoans and encrusting foraminifera.

DISCUSSION

Biostratigraphic Considerations

The benthic foraminiferal association determined in Rebaldí and the Benitatxell Range corresponds to the Shallow Benthic Zone (SBZ) 23, late Chattian, defined by the range of *Miogypsinoides complanatus* and *Miogypsinoides formosensis* (Cahuzac and Poignant 1997). Other taxa characteristic of this zone are *Eulepidina raulini*, *Eulepidina elephantina*, and *Risananeiza pustulosa*, while taxa with a longer stratigraphical range such as *Eulepidina dilatata*, *Amphistegina bohdanowiczi*, *Operculina complanata*, *Heterostegina assilinoides*, *Spiroclypeus blanckenhorni*, *Neorotalia viennoti*, and *Neorotalia lithothamnica* are also common in the biozone. The large variability of *Nephrolepidina*, together with the difficulty to obtain accurate measurements from thin sections precludes a specific assignment. The presence of *Amphistegina mammilla* and *Schlumbergerina alveoliniformis* in the late Chattian is reported for the first time. Previously, the first occurrence of *Amphistegina mammilla* in the western Tethys was placed in the middle Miocene (e.g., Popescu and Crihan 2008; Rögl and Brandstätter 1993), while the earliest occurrence of *Schlumbergerina alveoliniformis* is reported in the Burdigalian of Iran (e.g., Daneshian and Yazdani 2006). Similarly, *Cycloclypeus mediterraneus* was supposed to become extinct at the end of SBZ 22B, being replaced, in the western Tethys by *Cycloclypeus eidae* in SBZ 23 (e.g., Laagland 1990). Its presence in SBZ 23 characterized in our sections suggests that this replacement was not synchronous in the western Tethys.

Based on the number of post-embryonic spiral chambers, *Miogypsinoides* is subdivided into successive chrono-species, ranging from the early SBZ 23 to the early SBZ 24 (*Miogypsinoides bantamensis-dehartii*) with a considerable stratigraphical overlap of the different chrono-species (Cahuzac and Poignant 1997; Amirshahkarami 2008). The presence of *Miogypsinoides complanatus* in the Rebaldí section and of *Miogypsinoides formosensis* in the Benitatxell Range suggests an early age for the former, also indicated by the smaller proloculus and/or test size in *Heterostegina assilinoides*, *Spiroclypeus blanckenhorni*, and *Risananeiza pustulosa*. The absence of

large lepidocyclinids (*Eulepidina*), *Operculina*, and *Nummulites* in Rebaldí might be due to facies differences.

Thus, the Rebaldí section is placed in the early SBZ 23 (late Chattian), and the Benitatxell Range in the late SBZ 23 (latest Chattian). For a more detailed biostratigraphical discussion see Ferràndez-Cañadell and Bover-Arnal (2017).

Depositional Model

The latest Chattian lepidocyclinid-bearing lithofacies belt is laterally continuous along the Benitatxell Range (Figs. 1, 2A). This lithostratigraphic unit with benthic foraminifera and coralline algae thins slightly and progressively towards the southwest (Fig. 14). Large-scale step-like structures or bulging of sedimentary bodies were not recognized from the aerial photographs. Accordingly, the depositional profile along the Benitatxell Range during the latest Chattian corresponded to a homoclinal ramp (Fig. 15). In this respect, ramp depositional profiles were common in Chattian carbonate systems worldwide (e.g., Brandano et al. 2009a, 2010, 2012; van Buchem et al. 2010; Bassi and Nebelsick 2010; Pomar et al. 2014, 2015; Shabafrooz et al. 2015).

Within the coralline algal beds with benthic foraminifera studied here, fossil biotas indicate a progressive increase in water depth in a southward direction, from Rebaldí to Albacete Road section (Figs. 1A, 4–6, 14). This fact also supports a homoclinal ramp depositional profile (Figs. 15, 16). For example, the higher abundances of the lagenid foraminifera *Lenticulina* and *Nodosaria*, which inhabited distal ramp environments within the lower photic and aphotic zones (e.g., Geel 2000; Romero et al. 2002), are found in the Albacete Road section (Fig. 5). Therefore, thinning of the latest Chattian lithostratigraphic unit analyzed in the Benitatxell Range towards the southwest would be indicative of basinward sediment starvation.

In Rebaldí, skeletal components indicative of tropical to subtropical shallow ramp settings are abundant (Figs. 6, 14, 15). Such biotas thriving in the upper photic zone (*sensu* Hottinger 1997) include *Austrotrillina asmariensis* (Fig. 13D), other miliolids (Fig. 11A), *Schlumbergerina alveoliniformis*, *Planorbulina* sp. (Fig. 13A), *Planorbulinella* sp. (Fig. 13B), *Praebullalveolina* aff. *oligocenica*, *Peneroplis thomasi* (Fig. 13C), *Sphaerogypsina* sp. (Fig. 13H), gypsinids, *Haddonia heissigi* (Fig. 13M), *Miniacina* sp., *Victoriella conoidea*, *Solenomeris* sp., *Carpenteria* sp. (Fig. 13L), textularids (Fig. 11A), fragments of green algae (Fig. 11C), and coral colonies (Fig. 11B), locally forming metric patch reefs.

Nowadays, miliolids and peneroplids live on seagrass and algae, between 0 and 30 meters water depth, in low-latitude restricted platform settings including lagoons (e.g., Hallock and Glenn 1986; Hottinger 1997; Beavington-Penney and Racey 2004). Seagrass meadows frequently occupied inner ramp settings in the Chattian (e.g., Brandano et al. 2009b; Pomar et al. 2014, 2015; Shabafrooz et al. 2015; Brandano 2016). In this respect, other seagrass dwelling foraminifera such as cibicidids, *Planorbulina* sp. (Fig. 13A), *Planorbulinella* sp. (Fig. 13B), *Praebullalveolina* aff. *oligocenica*, and *Schlumbergerina alveoliniformis,* were also recognized in the rocks from Rebaldí (Figs. 6, 15). For example, Recent *Schlumbergerina alveoliniformis* thrives in vegetated areas, such as lagoons in tropical coral reefs, mostly between 0 and 20 meters water depth (Hofker 1971; Brasier 1975; Haig 1988; Langer and Lipps 2003). The encrusting foraminifera *Sphaerogypsina* sp. (Fig. 13H), gypsinids, *Haddonia heissigi* (Fig. 13M), *Miniacina* sp., *Victoriella conoidea*, *Solenomeris* sp., and *Carpenteria* sp. (Fig. 13L) identified in Rebaldí also indicate low-latitude upper photic zone environments (e.g., Romero et al. 2002; Brandano et al. 2009b), commonly associated with coral-bearing facies (e.g., Bosellini and Papazzoni 2003).

Lepidocyclinids, which were widespread in middle to outer ramp settings (e.g., Beavington-Penney and Racey 2004; Bassi and Nebelsick 2010; van Buchem et al. 2010; Brandano 2016), below ~ 40 meters water depth (Hottinger 1997), are rare in Rebaldí with only few abraded *Nephrolepidina* specimens recognized (Fig. 6). The deeper-water lepidocyclinid *Eulepidina* (e.g., Buxton 1988; Schiavinotto and Verrubbi 1994; Fenero et al. 2013), as well as *Nummulites* or *Operculina* sp., which nowadays inhabit the lower photic zone (e.g., Hohenegger et al. 2000; Beavington-Penney and Racey 2004), are absent (Fig. 6). *Cycloclypeus*, which is also a common deeper water foraminifer (Hottinger 1997; Beavington-Penney and Racey 2004), is also rare (Fig. 6).

The latest Chattian benthic foraminiferal assemblage determined in the Benitatxell Range, which includes lepidocyclinids, as well as other perforate foraminifera (Figs. 4, 5, 9), is characteristic of more distal ramp environments with respect to the biofacies characterized in Rebaldí (e.g., Hottinger 1997; Beavington-Penney and Racey 2004; Brandano et al. 2009b, 2012; Pomar et al. 2014; Brandano 2016). However, in Torre Garcia-Cim del Sol road section, from meter 94 to meter 104 (Fig. 4), colonial corals in growth position, fragments of green algae, *Peneroplis*, *Austrotrillina*, and abundant other miliolids occur. Furthermore, within this coral-bearing stratigraphic interval, the lepidocyclinid *Eulepidina*, which inhabited deeper habitats than that occupied by *Nephrolepidina* (Buxton 1988; Schiavinotto and Verrubbi 1994; Fenero et al. 2013), disappears. These beds with corals, also observed in the Accés Sud Road section (Fig. 5), recorded the progradation of proximal ramp facies above *Eulepidina*-bearing more distal ramp deposits (Figs. 14–16).

Outcrops showing lateral transitions from shallower ramp facies to deeper ramp and hemipelagic deposits were not found in the study area. Nevertheless, in Torre Garcia-Cim del Sol Road section, regressive late Chattian marl and limestone with echinoids and planktonic foraminifera are overlain by prograding latest Chattian coralline algal platform carbonates with lepidocyclinids (Fig. 14). Giving that both lithostratigraphic units belong to a same regressive genetic type of deposit, Walter's Law was applied (Figs. 15, 16), and the shallower ramp lepidocyclinid-bearing facies are interpreted to pass laterally to deeper ramp and hemipelagic deposits made up of alternating marl and limestone with echinoids, *Globigerinoides* and *Globigerina*.

Symbiont-bearing benthic foraminifera, such as nummulitids, amphisteginids, lepidocyclinids, and larger rotaliids, are also characteristic of tropical to subtropical carbonate systems (e.g., Betzler et al. 1997; Hohenegger 1999; Langer and Hottinger 2000). Therefore, the Chattian biotic assemblage preserved in the rocks exposed along the Benitatxell Range and Rebaldí evidences that carbonate sedimentation took place in tropical to subtropical marine waters.

Relative abundance of different coralline algal taxa can also be related with both water depth and latitude (see a recent review in Aguirre et al. 2016). Thus, melobesioids dominate the algal assemblages in high latitudes as well as in deep waters of low latitudes (Braga and Aguirre 2001, 2004; Braga et al. 2009). Sporolithales are abundant in deep waters at low latitudes, although they can be also found in shallow waters but in crevices and cryptic habitats (e.g., Braga and Bassi 2007). In this context, dominance of the melobesioids *Lithothamnion* and *Mesophyllum*, followed by *Sporolithon*, indicates that the studied deposits were mainly formed in middle to proximal outer platform settings as it has been inferred in other Oligocene Tethyan basins (e.g., Bassi and Nebelsick 2010; Braga and Bassi 2011; Brandano 2016). The bathymetric distribution of these taxa agrees with the paleoenvironmental conditions interpreted from benthic foraminifera, such as lepidocyclinids, *Heterostegina*, *Operculina*, or *Cycloclypeus*

(middle to proximal outer ramp settings; e.g., Beavington-Penney and Racey 2004; van Buchem et al. 2010; Brandano 2016).

High encrustation, bioerosion, abrasion, and fragmentation of skeletal components, as well as the occurrence of rhodoliths (Figs. 4–6, 7C), are indicative of slow sedimentation rates. This implies moderate to prolonged time of residence on the sea floor for the biogenic material examined. On the other hand, pre-burial taphonomic features, such as fragmentation and abrasion, are also good sediment-transport indicators (e.g., Beavington-Penney 2004). In this respect, skeletal components occur highly fragmented and abraded in the rocks studied in both Rebaldí and the Benitatxell Range (Figs. 4–6, 10C, 10D, 11A). According to Beavington-Penney (2004), the levels of abrasion displayed by the nummulitid foraminifera examined indicate moderate, extensive and turbiditic transport with wave re-working, and/or predation by large bioeroders. Therefore, taphonomic attributes could be also in accordance with intense re-mobilization of skeletal components throughout the ramp. In this respect, the facies in Rebaldí and Benitatxell Range is quite homogeneous. Biota from different ramp environments are mixed in the deposits studied (Figs. 4–6). Probably, the most remarkable difference between the late Chattian platform carbonates found in Rebaldí and the latest Chattian ramp deposits of the Benitatxell Range (Figs. 4, 5), is the absence of *Eulepidina*, *Nummulites*, and *Operculina* in the first locality (Fig. 6), which highlights bathymetric differences (Fig. 15). Owing to mixing of biota, upper/lower photic or euphotic/oligophotic and aphotic divisions were not included in the ramp model (Fig. 15).

The absence of hydrodynamic structures or important textural variations in such re-worked carbonates dominated by benthic foraminifera and coralline algae is conspicuous. The formation of sedimentary structures relies on the presence of subtle grain size contrasts (Jorry et al. 2006). Therefore, the important differences in size of the skeletal components in the analyzed rocks (Figs. 7A, 7C, 7D, 10, 11) could have hindered the potential formation of sedimentary structures generated by water motion. Accordingly, the resulting ramp model (Fig. 15) is not sub-divided into inner, middle, and outer parts. This latter sub-division is related to hydrodynamic conditions (Burchette and Wright 1992).

Depositional Architecture and Sequence Stratigraphy

The latest Chattian platform carbonates with coralline algae and benthic foraminifera studied in the Benitatxell Range are encased between an underlying marly unit with intercalated limestone beds, and an overlying succession formed by marl and silty to sandy limestone (Figs. 4, 14). Both marl-bearing successions are rich in planktonic foraminifera and glauconite. Furthermore, the limestone beds alternating with marl of the lower part of the Torre Garcia-Cim del Sol Road section (Fig. 2C) have been interpreted as a flysch succession by Vegas et al. (1973) and Lendínez Gonzalez et al. (1993). The marl lithology, as well as the occurrence of turbidite beds, and of abundant planktonic foraminifera, mainly globigerinids, support deposition in deeper-water conditions than the coralline algal limestone with benthic foraminifera investigated (e.g., Hallock and Glenn 1986; Geel 2000; van Buchem et al. 2010; Bassi et al. 2013). Along the same lines, relatively high concentrations of glauconite are commonly linked to transgressive contexts and maximum flooding events (e.g., Amorosi and Centineo 1997; Huggett and Gale 1997; Wigley and Compton 2007).

In the Rebaldí section, the late Chattian coralline algal limestones with benthic foraminifera overlay unconformably Cretaceous rocks (Figs. 3E, 14, 16). The origin of this angular unconformity, which has a regional significance, and locally bounds tilted Eocene deposits (below) from Oligocene strata (above) (Geel 1995), is not clear

(Moseley 1990). It could be related to a compressional phase accompanied by uplift of late Eocene–early Oligocene age linked to the Pyrenean collision (Fontboté et al. 1990; Geel 1995; Stoklosa and Simo 2008). This unconformity was inspected in the Rebaldí section (Figs. 3E, 6, 14), and signs of prolonged subaerial exposure, such as paleokarst, paleosol, or vadose cement fabrics, were not observed. However, Geel (1995) reported the occurrence of middle Rupelian karst features in the area, as well as of *Paronipora* (=*Microcodium*) on top of the Cretaceous substrate, and below Chattian carbonates, in nearby outcrops located about 15 km to west. In addition, up to tens-of-meters thick conglomerate deposits with clasts of diverse ages, mainly Paleocene, are locally present overlying this unconformity (Vegas et al. 1973). This implies that a topographic high existed or emerged during the late Eocene–early Oligocene. Therefore, short-lived subaerial exposure conditions resulting in surficial erosion during this time interval seem plausible.

The unconformity between the Cretaceous substrate and the Cenozoic succession is thus interpreted as a sequence boundary, which marks the base of Sequence I (Figs. 14, 16). Above, a marine transgression of Oligocene age flooded the irregular paleotopographic relief shaped on the Cretaceous substrate (Figs. 14, 16). The Oligocene transgressive sedimentary fill onlaps the sequence boundary. The transgressive succession examined in the Rebaldí section is formed by platform carbonates with benthic foraminifera and coralline algae (Fig. 6), which were deposited on a paleotopographic high (Figs. 14, 16). In the Benitatxell Range, the transgressive strata correspond to deeper-water marl and limestone with echinoids, planktonic foraminifera and glauconite (Figs. 2C, 4, 14, 16).

The end of transgression was placed in the Rebaldí section below upper Chattian platform carbonates stacked in a prograding pattern and exhibiting downlap stratal terminations (Figs. 3D, 14). In the Benitatxell Range, the maximum flooding surface is located at the top of the thickest marl interval, which is interpreted to indicate the greatest amount of depositional space attained during transgression (Fig. 14).

Above the maximum flooding surface, the regressive deposits of Sequence I in Rebaldí are distinguished by prograding carbonates (Fig. 3D) with colonial corals in life position, benthic foraminifera and coralline algae (Figs. 6, 11B, 12, 13). At the top of these regressive strata, the occurrence of *Paronipora* (=*Microcodium*) structures (Figs. 3D, 6, 11D, 14, 16) indicates subaerial exposure conditions (e.g., Kabanov et al. 2008). Accordingly, a subaerial unconformity (sequence boundary), which passes basinwards to a maximum regressive surface (Figs. 14, 16), caps the platform carbonate succession of the Rebaldí section.

In the Benitatxell Range, the lower part of the regressive unit of Sequence I is characterized by an alternation of marl and limestone with planktonic foraminifera and echinoids (Figs. 14, 16). The deposits show a progressive vertical increase in the abundance of re-worked symbiont-bearing benthic foraminifera between meters 65 and 82 in the Torre Garcia-Cim del Sol Road section (Fig. 4). This fact indicates a gradual increase of shed sediments from a nearby prograding carbonate platform and thus, a shallowing-upward trend. Above, regressive lepidocyclinid-bearing platform carbonates constitute the rest of the regressive strata (Figs. 4, 14). Evidence of subaerial exposure was not identified within these latest Chattian limestones in the Benitatxell Range. Therefore, the upper boundary of Sequence I is interpreted to be a maximum regressive surface, which was placed at the top of beds containing fossil biota representative of the shallowest environments recognized throughout the successions studied (Fig. 14). In the Torre Garcia-Cim del Sol Road section, which corresponds to the most proximal section logged in the Benitatxell Range, the maximum regressive surface is interpreted to be

located at meter 104. Here, this surface surmounts a 10-m thick succession characterized by the presence of colonial corals in growth position, fragments of green algae, *Peneroplis*, *Austrotrillina*, and abundant other miliolids. Such biotas are usually found in shallow proximal platform settings (e.g., Hottinger 1997; Geel 2000; van Buchem et al. 2010; Pomar et al. 2014). Furthermore, along this coral-bearing stratigraphic interval (between meters 94 and 104; Fig. 4), the lepidocyclinid genus *Eulepidina* (Figs. 7A, 9B, 9C), which thrived in deeper-water settings with respect to *Nephrolepidina* (Fig. 7B) (e.g., Buxton 1988; Schiavinotto and Verrubbi 1994; Fenero et al. 2013), disappears. In the Accés Sud Road section, the maximum regressive surface was placed at meter 7 (Figs. 5, 14), above the only bed containing corals in growth position identified, whereas in the Albacete Road section, this limit is not clear. However, it is tentatively placed at the top of a bed containing fragments of green algae (meter 14; Figs. 5, 14).

Above the maximum regressive surface, the platform carbonates are dominated by echinoids, coralline algae and benthic foraminifera (Figs. 4, 5, 14). In the Torre Garcia-Cim del Sol Road section, the lepidocyclinid *Eulepidina* (Figs. 7A, 9B, 9C) reappears at meter 113, and becomes a facies-characteristic component between meters 120 and 124 (Fig. 4). This fact, together with the increase and decrease in the abundance of planktonic foraminifera and coralline algae, respectively, and the presence of *Nodosaria* and *Lenticulina* (Fig. 4), which are common in distal platform settings (Fig. 15; e.g., Geel 2000; Romero et al. 2002), mark a deepening-upwards trend (Figs. 14, 16). Accordingly, these carbonates form the transgressive unit of Sequence II (Figs. 14, 16). On the course of the marine transgression of Sequence II, the latest Chattian carbonate platform with coralline algae and benthic foraminifera was drowned, and subsequently buried by a lower Miocene succession of marl and silty to sandy limestone with planktonic foraminifera and glauconite (Figs. 3F, 4, 5, 14, 16).

As a result, the analyzed Chattian lepidocyclinid limestones recorded a regression of relative sea level between two major transgressions, one starting in the Rupelian?–early Chattian and ending in the late Chattian, and the other one initiating in the latest Chattian and continuing into the early Miocene (Figs. 14, 16). This regression occurred within the late Chattian SBZ 23. The duration estimate for the Chattian Age is 5.1 My (Gradstein et al. 2012). Therefore, the regressive stage of Sequence I occurred in much less than 5.1 My.

The duration of the relative sea-level changes recognized in Rebaldí and the Benitatxell Range is less than the resolution of the age constraints obtained by means of benthic foraminifera biostratigraphy. Furthermore, the marly units overlying and underlying the calibrated lepidocyclinid limestone did not yield symbiont-bearing benthic foraminifera (Figs. 4, 5), and were therefore not dated as accurately as the lepidocyclinid limestone assigned to the late Chattian SBZ 23. In addition, the amplitude of the relative sea-level fluctuations interpreted is unknown. Hence, rates of relative sea-level change were not estimated in the successions analyzed.

Geel (1995) reported for the Rebaldí-Benitatxell Range area a late Rupelian–late Chattian phase of downwarp, an episode of tectonic uplift in the late Chattian, followed by a downwarp phase starting around the Oligocene/Miocene transition and continuing into the Aquitanian. Following Geel (1995), regional tectonic activity linked to the Pyrenean and Betic orogenies (Azéma 1977; Roca 1992), and possibly to the rifting of the València Trough (Fontboté et al. 1990), explains the relative sea-level changes recognized. On the other hand, early to late Chattian and early Miocene transgressions, as well as late to latest Chattian regressive deposits have been documented in several other basins of the Tethys (e.g., Hardenbol et al. 1998). Therefore, eustasy could have

also played a part in controlling these long-term transgressive-regressive sequences identified.

The correlation between the resulting sequence-stratigraphic framework and that obtain by Hardenbol et al. (1998) from the European basins of the Tethys does not show a perfect fit. According to Hardenbol et al. (1998), the acme of the late Chattian regression in the Tethys occurred in the Chattian/Aquitanian transition coinciding with the Mi-1 glaciation (e.g., Zachos et al. 2001; Mudelsee et al. 2014), whereas the onset of the following transgression was in the Aquitanian. The age-calibration of the outcrops studied in Rebaldí and the Benitatxell Range indicates that here, the maximum regressive phase identified and the earliest stage of the subsequent transgression took place within the latest Chattian SBZ 23 (Figs. 14, 16). Accordingly, the effects of regional tectonics seem to have slightly altered the eustatic signal (e.g., Hardenbol et al. 1998) in the study area.

On the other hand, drowning of the carbonate system of the Benitatxell Range occurred indeed around the boundary between the Chattian and the Aquitanian (Fig. 14). Interestingly, drowning of latest Chattian carbonate platforms during the Chattian/Aquitanian transition has been also reported in the Central Apennines in Italy (Majella platform; Brandano et al. 2015) or in Malta (Lower Coralline Limestone Formation; Brandano et al. 2009a).

CONCLUSIONS

The carbonate system studied, which developed under warm, tropical to subtropical conditions during the Chattian, is very similar in terms of biofacies and depositional profile to contemporaneous carbonate platforms from the Tethys. It was a homoclinal ramp and the most prolific carbonate producers were symbiont-bearing benthic foraminifera and coralline algae.

A biostratigraphic analysis based on benthic foraminifera places these platform carbonates within the late Chattian Shallow Benthic Zone (SBZ) 23. Age-diagnostic foraminifera of SBZ 23 determined include *Miogypsinoides complanatus* and *Miogypsinoides formosensis*.

The only authochthonous carbonates recognized in the rocks studied are colonies of wholly preserved scleractinians in growth position, which occur isolated or as small coral patch reefs, found in proximal ramp deposits. In this Chattian carbonate system, scleractinian corals did not build large wave-resistant framework structures with topographic relief such as Recent tropical and subtropical barrier reefs. Other types of barrier deposits such as shoals were not recognized and thus, the platform lacked a lagoon.

The absence of a barrier margin facilitated onshore and offshore sediment export and re-working throughout the platform, while homogenizing the facies from proximal to distal ramp settings. In this respect, the overwhelming dominant and extensive facies produced was a rudstone texture mainly made up of benthic foraminifera and coralline algae with micrite filling the primary inter- and intraskeletal porosity. Accordingly, strongly different facies belts delimitated by rather sharp boundaries along the carbonate platform examined were not identified, only little and gradual lateral variations on the relative abundance or absence of certain biogenic components or species can be recognized.

Thus, the limestones analyzed exemplify that carbonates found in the sedimentary record are commonly made up of re-worked sediments transported from different platform environments. However, within this facies dominated by benthic foraminifera and coralline algae two end members were identified: a shallower biofacies

including corals in growth position, green algae, and seagrass-related organisms where *Eulepidina*, *Nummulites*, and *Operculina* are not present, and vice versa.

Long-term relative sea-level changes including a Rupelian?–late Chattian transgression, a late Chattian regression, which ended in subaerial exposure of inner platform carbonates, and a latest Chattian to early Miocene transgression were identified. These long-term trends of relative sea level are slightly out of phase when correlated to coeval transgressive-regressive cycles characterized in other basins of the Tethys. Hence, regional tectonics linked to the Pyrenean and Betic orogenies, and perhaps also to the opening of the València Trough, is interpreted to have played a part in controlling available depositional space in the Prebetic Zone during this time. Drowning of the Chattian carbonate platform around the Oligocene/Miocene transition was contemporaneous to the Mi-1 glaciation.

ACKNOWLEDGMENTS

This study is part of an initiative of Repsol Exploración S.A. to support research at the Faculty of Geology of the University of Barcelona. This logistic and financial support is greatly acknowledged. Alejandro Gallardo and Alia Ponz are thanked for laboratory and field assistance, respectively. Eduard Roca provided valuable information on the geological setting. Comments by two anonymous reviewers improved the manuscript. Complementary funding by the Grup de Recerca Reconegut per la Generalitat de Catalunya 2014 SGR 251 "Geologia Sedimentària" and the I + D + i research projects CGL2015-60805-P (BIOGEOEVENTS) and CGL2013-47236-P are appreciated.

REFERENCES

AGUIRRE, J., BRAGA, J.C., and BASSI, D., 2016, Rhodolith and rhodolith beds in the rock record, *in* R. Riosmena-Rodríguez, W. Nelson, and J. Aguirre (eds.), Rhodolith/Maerl beds: A Global Perspective: Springer International Publishing, Coastal Research Library, v. 15, p. 105–138.

ALEGRET, L., CRUZ, L.E., FENERO, R., MOLINA, E., ORTIZ, S., and THOMAS, E., 2008, Effects of the Oligocene climatic events on the foraminiferal record from Fuente Caldera section (Spain, western Tethys): Palaeogeography, Palaeoclimatology, Palaeoecology, v. 269, p. 94–102.

AMOROSI, A. and CENTINEO, M.C., 1997, Glaucony from the Eocene of the Isle of Wight (southern UK): implications for basin analysis and sequence-stratigraphic interpretation: Journal of the Geological Society, London, v. 154, p. 887–896.

AZÉMA, J., 1977, Étude géologique des zones externes des cordillères bétiques aux confins des provinces d'Alicante et de Murcie (Espagne): Ph.D. thesis, Université Pierre et Marie Curie, Paris, 396 p.

BANERJEE, A., YEMANE, K., and JOHNSON, A., 2000, Foraminiferal biostratigraphy of late Oligocene–Miocene reefal carbonates in southwestern Puerto Rico: Micropaleontology, v. 46, p. 327–342.

BASSI, D., HOTTINGER, L., and NEBELSICK, J.H., 2007, Larger foraminifera from the upper Oligocene of the Venetian area, north-east Italy: Palaeontology, v. 50, p. 845–868.

BASSI, D. and NEBELSICK, J.H., 2010, Components, facies and ramps: redefining upper Oligocene shallow water carbonates using coralline red algae and larger foraminifera (Venetian area, northeast Italy): Palaeogeography, Palaeoclimatology, Palaeoecology, v. 295, p. 258–280.

BASSI, D., NEBELSICK, J.H., PUGA-BERNABÉU, Á., and LUCIANI, V., 2013, Middle Eocene *Nummulites* and their offshore re-deposition: a case study from the

middle Eocene of the Venetian area, northeastern Italy: Sedimentary Geology, v. 297, p. 1–15.

BEAVINGTON-PENNEY, S.J., 2004, Analysis of the effects of abrasion on the test of *Palaeonummulites venosus*: implications for the origin of nummulithoclastic sediments: PALAIOS, v. 19, p. 143–155.

BEAVINGTON-PENNEY, S.J. and RACEY, A., 2004, Ecology of extant nummulitids and other larger benthic foraminifera: applications in palaeoenvironmental analysis: Earth-Science Reviews, v. 67, p. 219–265.

BEHFOROUZI, E. and SAFARI, A., 2011, Biostratigraphy and paleoecology of the Qom Formation in Chenar area (northwestern Kashan), Iran: Revista Mexicana de Ciencias Geológicas, v. 28, p. 555–565.

BERNING, B., REUTER, M., PILLER, W.E., HARZHAUSER, M., and KROH, A., 2009, Larger foraminifera as a substratum for encrusting bryozoans (late Oligocene, Tethyan Seaway, Iran): Facies, v. 55, p. 227–241.

BETZLER, C., BRACHERT, T.C., and NEBELSICK, J., 1997, The warm temperate carbonate province, a review of the facies, zonations and delimitations: Courier Forschungsinstitut Senckenberg, v. 201, p. 83–99.

BOSELLINI, F.R. and PAPAZZONI, C.A., 2003, Palaeoecological significance of coral-encrusting foraminiferan associations: a case-study from the upper Eocene of northern Italy: Acta Palaeontologica Polonica, v. 48, p. 279–292.

BOSENCE, D.W.J., 1976, Ecological studies on two unattached coralline algae from western Ireland: Palaeontology, v. 19, p. 365–395.

BOSENCE, D.W.J., 1983, Description and classification of rhodoliths (rhodoids, rhodolites), *in* T.M. Peryt (ed.), Coated Grains: Springer-Verlag, Berlin, p. 217–224.

BOUKHARY, M., KUSS, J., and ABDELRAOUF, M., 2008, Chattian larger foraminifera from Risan Aneiza, northern Sinai, Egypt, and implications for the Tethyan paleogeography: Stratigraphy, v. 5, p. 179–192.

BRAGA, J.C. and AGUIRRE, J., 2001, Coralline algal assemblages in upper Neogene reef and temperate carbonates in Southern Spain: Palaeogeography, Palaeoclimatology, Palaeoecology, v. 175, p. 27–41.

BRAGA, J.C. and AGUIRRE, J., 2004, Coralline algae indicate Pleistocene evolution from deep, open platform to outer barrier reef environments in the northern Great Barrier Reef margin: Coral Reefs, v. 23, p. 547–558.

BRAGA, J.C. and BASSI, D., 2007, Neogene history of *Sporolithon* Heydrich (Corallinales, Rhodophyta) in the Mediterranean region: Palaeogeography, Palaeoclimatology, Palaeoecology, v. 243, p. 189–203

BRAGA, J.C. and BASSI, D., 2011, Facies and coralline algae from Oligocene limestones in the Malaguide Complex (SE Spain): Annalen des Naturhistorischen Museums in Wien, Serie A, v. 113, p. 291–308.

BRAGA, J.C., MARTÍN, J.M., and AGUIRRE, J., 2002, Tertiary. Southern Spain, *in* W. Gibbons and T. Moreno (eds.), The Geology of Spain: The Geological Society, London, p. 320−327.

BRAGA, J.C., VESCOGNI, A., BOSELLINI, F., and AGUIRRE, J., 2009, Coralline algae in Mediterranean Messinian reefs: Palaeogeography, Palaeoclimatology, Palaeoecology, v. 275, p. 113–128.

BRANDANO, M., 2016, Oligocene Rhodolith beds in the Central Mediterranean area, *in* R. Riosmena-Rodríguez, W. Nelson, and J. Aguirre (eds.), Rhodolith/Maerl Beds: A Global Perspective: Springer International Publishing, Coastal Research Library, v. 15, p. 195–219.

BRANDANO, M., FREZZA, V., TOMASSETTI, L., and CUFFARO, M., 2009b, Heterozoan carbonates in oligotrophic tropical waters: the Attard member of the lower coralline limestone formation (upper Oligocene, Malta): Palaeogeography, Palaeoclimatology, Palaeoecology, v. 274, p. 54–63.

BRANDANO, M., FREZZA, V., TOMASSETTI, L., PEDLEY, M., and MATTEUCCI, R., 2009a, Facies analysis and palaeoenvironmental interpretation of the late Oligocene Attard Member (Lower Coralline Limestone Formation), Malta: Sedimentology, v. 56, p. 1138–1158.

BRANDANO, M., LIPPARINI, L., CAMPAGNONI, V., and TOMASSETTI, L., 2012, Downslope-migrating large dunes in the Chattian carbonate ramp of the Majella Mountains (Central Apennines, Italy): Sedimentary Geology, v. 255–256, p. 29–41.

BRANDANO, M., LUSTRINO, M., CORNACCHIA, I., and SPROVIERI, M., 2015, Global and regional factors responsible for the drowning of the Central Apennine Chattian carbonate platforms: Geological Journal, v. 50, p. 575–591.

BRANDANO, M., MORSILI, M., VANNUCCI, G., PARENTE, M., BOSELLINI, F., and MATEU-VICENS, G., 2010, Rhodolith-rich lithofacies of the Porto Badisco Calcarenites (upper Chattian, Salento, southern Italy): Italian Journal of Geosciences, v. 129, p. 119–131.

BRASIER, M.D., 1975, An outline history of seagrass communities: Palaeontology, v. 18, p. 681–702.

BURCHETTE, T.P. and WRIGHT, V.P., 1992, Carbonate ramp depositional systems: Sedimentary Geology, v. 79, p. 3–57.

BUXTON, M.W.N., 1988, Morphology and habitat of upper Oligocene Lepidocyclinids from the Maltese Islands: Revue de Paléobiologie, Spécial v. 2, p. 631–632.

CAHUZAC, B. and POIGNANT, A., 1997, Essai de biozonation de l'Oligo-Miocène dans les bassins européens à l'aide des grands foraminifères néritiques: Bulletin de la Société Géologique de France, v. 168, p. 155–169.

CATUNEANU, O., GALLOWAY, W.E., KENDALL, C.G.ST.C., MIALL, A.D., POSAMENTIER, H.W., STRASSER, A. and TUCKER, M.E., 2011, Sequence stratigraphy: methodology and nomenclature: Newsletters on Stratigraphy, v. 44, p. 173–245.

CHECCONI, A. and MONACO, P., 2008, Trace fossil assemblages in rhodoliths from the middle Miocene of Mt. Camposauro (Longano Formation, Southern Apennines, Italy): Studi Trentini di Scienze Naturali, Acta Geologica, v. 83, p. 165–176.

COSICO, R., GRAMANN, F., and PORTH, H., 1989, Larger foraminifera from the Visayan Basin and adjacent areas of the Philippines (Eocene through Miocene): Geologisches Jahrbuch, v. 70, p. 147–205.

ĆOSOVIĆ, V., DROBNE, K., and IBRAHIMPAŠIĆ, H., 2012, The role of taphonomic features in the palaeoecological interpretation of Eocene carbonates from the Adriatic carbonate platform (PgAdCP): Neues Jahrbuch für Geologie und Paläontologie–Abhandlungen, v. 265, p. 101–112.

DANESHIAN, J. and Yazdani, H., 2006, A study of stratigraphic distribution of benthonic foraminifera from Qom Formation in West Saveh: Quarterly Research Journal of University of Isfahan "Science", v. 25, no. 3, p. 13–28, http://egeology.blogfa.com/87123.aspx?p=15. (In Persian)

DERCOURT, J., GAETANI, M., VRIELYNCK, B., BARRIER, E., BIJU-DUVAL, B., BRUNET, M.F., CADET, J.P., CRASQUIN, S., and SANDULESCU, M., 2000, Atlas Peri-Tethys, palaeogeographical maps: CCGM/CGMW, Paris.

DUNHAM, R.J., 1962, Classification of carbonate rocks according to depositional texture, *in* W.E. Ham (ed.), Classification of Carbonate Rocks: AAPG Memoir, v. 1, p. 108–121.

ELLIOTT, G.F., 1960, Fossil calcareous algal floras of the Middle East with a note on a Cretaceous problematicum, *Hensonella cylindrical* gen. et sp. nov.: Quarterly Journal of the Geological Society of London, v. 3, p. 217–232.

EMBRY, A.F. and KLOVAN, J.E., 1971, A Late Devonian reef tract on northeastern Banks Island, N.W.T: Bulletin of Canadian Petroleum Geology, v. 19, p. 730–781.

FENERO, R., COTTON, L., MOLINA, E., and MONECHI, S., 2013, Micropalaeontological evidence for the late Oligocene Oi-2b global glaciation event at the Zarabanda section, Spain: Palaeogeography, Palaeoclimatology, Palaeoecology, v. 369, p. 1–13.

FERRÀNDEZ-CAÑADELL, C. and BOVER-ARNAL, T., 2017, Late Chattian larger foraminifera from the Prebetic Domain (SE Spain), new data on shallow benthic zone 23: PALAIOS, v. 32, p. xxx–xxx.

FONTBOTÉ, J.M., GUIMERÀ, J., ROCA, E., SÀBAT, F., SANTANACH, P., and FERNÁNDEZ-ORTIGOSA, F., 1990, The Cenozoic geodynamic evolution of the València Trough (western Mediterranean): Revista de la Sociedad Geológica de España, v. 3, p. 249–259.

FOURNIER, F., BORGOMANO, J., and MONTAGGIONI, L.F., 2005, Development patterns and controlling factors of Tertiary carbonate buildups: Insights from high-resolution 3D seismic and well data in the Malampaya gas field (Offshore Palawan, Philippines): Sedimentary Geology, v. 175, p. 189–215.

FOURNIER, F., MONTAGGIONI, L.F., and BORGOMANO, J., 2004, Paleoenvironments and high-frequency cyclicity from Cenozoic South-East Asia shallow-water carbonates: a case study from the Oligo-Miocene buildups of Malampaya (Offshore Palawan, Philippines): Marine and Petroleum Geology, v. 21, p. 1–21.

FRAVEGA, P., PIAZZA, M., STOCKAR, R., and VANNUCCI, G., 1994, Oligocene coral and algal reef and related facies of Valzemola (Savona, NW Italy): Rivista Italiana di Paleontologia e Stratigrafia, v. 100, p. 423–456.

GARCÍA-HERNÁNDEZ, M., LÓPEZ-GARRIDO, A.C., RIVAS, P., SANZ DE GALDEANO, C., and VERA, J.A., 1980, Mesozoic palaeogeographic evolution of the external zones of the Betic Cordillera: Geologie en Mijnbouw, v. 52, p. 155–168.

GEEL, T., 1995, Oligocene to early Miocene tectono-sedimentary history of the Alicante region (SE Spain): implications for the Western Mediterranean evolution: Basin Research, v. 7, p. 313–336.

GEEL, T., 1996, Palaeogene to early Miocene sedimentary history of the Sierra Espuña (Malaguide complex, internal zone of the Betic cordilleras, SE Spain), evidence for extra-Malaguide (Sardinian?) provenance of Oligocene conglomerates: palaeogeographic implications: Estudios Geológicos, v. 52, p. 211–230.

GEEL, T., 2000, Recognition of stratigraphic sequences in carbonate platform and slope deposits: empirical models based on microfacies analysis of Palaeogene deposits in southeastern Spain: Palaeogeography, Palaeoclimatology, Palaeoecology, v. 155, p. 211–238.

GEEL, T., ROEP, T.B., and VAN HINTE, J.E., 1998, Eocene tectono-sedimentary patterns in the Alicante Region (southeastern Spain), *in* P.C. de Graciansky, J. Hardenbol, T. Jaquin, and P.R. Vail (eds.), Mesozoic and Cenozoic sequence stratigraphy of European basin: SEPM Special Publication, v. 60, p. 289–302.

GRADSTEIN, F.M., OGG, J.G., SCHMITZ, M.D., and OGG, G.M., 2012, The Geologic Time Scale 2012: Elsevier, Oxford, 1144 p.

HAIG, D.W., 1988, Miliolid foraminifera from inner neritic sand and mud facies of the Papuan lagoon, New Guinea: Journal of Foraminiferal Research, v. 18, p. 203–236.

HALLOCK, P. and GLENN, E.C., 1986, Larger foraminifera: a tool for paleoenvironmental analysis of Cenozoic carbonate depositional facies: PALAIOS, v. 1, p. 55–64.

HARDENBOL, J., THIERRY, J., FARLEY, M.B., JACQUIN, T., DE GRACIANSKI, P.C., and VAIL, P.R., 1998, Mesozoic and Cenozoic Sequence Chronostratigraphic Framework of European Basins, *in* P.C. de Graciansky, J. Hardenbol, T. Jacquin, and P.R. Vail (eds.), Mesozoic and Cenozoic Sequence Stratigraphy of European Basins: SEPM Special Publication, v. 60, p. 3–13, charts 1–8.

HOFKER, J., 1971, The foraminifera of Piscadera Bay, Curaçao: studies on the fauna of Curaçao and other Caribbean islands: Caribbean Marine Biological Institute, v. 35, p. 1–62.

HOHENEGGER, J., 1999, Larger foraminifera—microscopical greenhouses indicating shallow-water tropical to subtropical environments in the present and the past: Kagoshima University Research Center for the Pacific Islands, Occasional Papers, v. 32, p. 19–45.

HOHENEGGER, J., YORDANOVA, E., and HATTA, A., 2000, Remarks on West Pacific Nummulitidae (Foraminifera): Journal of Foraminiferal Research, v. 30, p. 3–28.

HÖNTZSCH, S., SCHEIBNER, C., BROCK, J.P., and KUSS, J., 2013, Circum-Tethyan carbonate platform evolution during the Palaeogene: the Prebetic platform as a test for climatically controlled facies shifts: Turkish Journal of Earth Sciences, v. 22, p. 891–918.

HOTTINGER, L., 1997, Shallow benthic foraminiferal assemblages as signals for depth of their deposition and their limitations: Bulletin de la Société Géologique de France, v. 168, p. 491–505.

HUGGETT, J. M. and GALE, A.S., 1997, Petrology and palaeoenvironmental significance of glaucony in the Eocene succession at Whitecliff Bay, Hampshire Basin, UK: Journal of the Geological Society, London, v. 154, p. 897–912.

INSALACO, E., 1998, The descriptive nomenclature and classification of growth fabrics in fossil scleractinian reefs: Sedimentary Geology, v. 118, p. 159–186.

IRYU, Y., INAGAKI, S., SUZUKI, Y., and YAMAMOTO, K., 2010, Late Oligocene to Miocene reef formation on Kita-daito-jima, northern Philippine Sea, *in* M. Mutti, W.E. Piller, and C. Betzler (eds.), Carbonate Systems During the Oligocene–Miocene Climatic Transition: International Association of Sedimentologists Special Publication, v. 42, p. 245–256.

IŞIK, U. and HAKYEMEZ, A., 2011, Integrated Oligocene−lower Miocene larger and planktonic foraminiferal biostratigraphy of the Kahramanmaraş Basin (Southern Anatolia, Turkey): Turkish Journal of Earth Sciences, v. 20, p. 185–212.

ITURRALDE-VINENT, M.A., 1972, Principal characteristics of Oligocene and lower Miocene stratigraphy of Cuba: AAPG Bulletin, v. 56, p. 2369–2379.

JEREZ-MIR, L., 1973, Geología de la Zona Prebética, en la transversal de Elche de la Sierra y sectores adyacentes (Provincias de Albacete y Murcia): Ph.D. thesis, University of Granada, 750 p.
JEREZ-MIR, L., 1981, Estudio geológico, geotectónico y tectonosedimentario de la Zona Prebética en relación con las demás Cordilleras Béticas e Ibérica: Informe Interno IGME, Madrid, 160 p.
JORRY, S.J., HASLER, C.-A., and DAVAUD, E., 2006, Hydrodynamic behaviour of *Nummulites*: implications for depositional models: Facies, v. 52, p. 221–235.
JURGAN, H., and DOMINGO, R.MA.A., 1989, Younger Tertiary limestone formations in the Visayan Basin, Philipines: Geologisches Jahrbuch, v. 70, p. 207–275.
KABANOV, P., ANADÓN, P., and KRUMBEIN, W.E., 2008, *Microcodium*: an extensive review and proposed non-rhizogenic biologically induced origin for its formation: Sedimentary Geology, v. 205, p. 79–99.
KAISER, D., RASSER, M.W., NEBELSICK, J.H., and PILLER, W.E., 2001, Late Oligocene algal limestones on a mixed carbonate-siliciclastic ramp at the southern margin of the Bohemian Massif (Upper Austria), *in* W.E. Piller and M.W. Rasser (eds.), Paleogene of the Eastern Alps: Österreichische Akademie der Wissenschaften, Schriftenreihe der Erdwissenschaftlichen Kommission, v. 14, p. 197–224.
KNOERICH, C.A. and MUTTI, M., 2003, Controls of facies and sediment composition on the diagenetic pathway of shallow-water Heterozoan carbonates: the Oligocene of the Maltese Islands: International Journal of Earth Sciences, v. 92, p. 494–510.
KUMAR, A. and SARASWATI, P., 1997, Response of larger foraminifera to mixed carbonate-siliciclastic environments: an example from the Oligocene–Miocene sequence of Kutch, India: Palaeogeography, Palaeoclimatology, Palaeoecology, v. 136, p. 53–65.
KUSS, J. and BOUKHARY, M.A., 2008, A new upper Oligocene marine record from the northern Sinai (Egypt) and its paleogeographic context: GeoArabia, v. 136, p. 53–65.
LAAGLAND, H, 1990, *Cycloclypeus* in the Mediterranean Oligocene: Utrecht Micropaleontological Bulletins, v. 39, p. 1–171.
LANGER, M. and HOTTINGER, L., 2000, Biogeography of selected 'larger' foraminifera: Micropaleontology, v. 46, p. 105–126.
LANGER, M.R. and LIPPS, J.H., 2003, Foraminiferal distribution and diversity, Madang Reef and Lagoon, Papua New Guinea: Coral Reefs, v. 22, p. 143–154.
LEAR, C.H., ELDERFIELD, H., and WILSON, P.A., 2000, Cenozoic deep-sea temperature and global ice volumes from Mg/Ca in benthic foraminiferal calcite: Science, v. 287, p. 269–272.
LENDÍNEZ GONZALEZ, A., MUÑOZ DEL REAL, J.L., and PASCUAL MUÑOZ, H., 1993, Benissa, hoja n° 822, mapa geológico de España 1:50.000: Servicio de Publicaciones, Ministerio de Industria, Madrid, 2ª Serie, 1ª Edición, 72 p.
MADDEN, R.H.C. and WILSON, M.E.J., 2013, Diagensis of a SE Asian Cenozoic carbonate platform margin and its adjacent basinal deposits: Sedimentary Geology, v. 286–287, p. 20–38.
MARTÍN-CHIVELET, J. and CHACÓN, B., 2007, Event stratigraphy of the upper Cretaceous to lower Eocene hemipelagic sequences of the Prebetic Zone (SE Spain): record of the onset of tectonic convergence in a passive continental margin: Sedimentary Geology, v. 197, p. 141–163.

MOSELEY, F., 1990, A geological field guide to the Costa Blanca, Spain: Geologists' Association Guide, The Geologists' Association, London, 79 p.

MUDELSEE, M., BICKERT, T., LEAR, C.H., and LOHMANN, G., 2014, Cenozoic climate changes: a review based on time series analysis of marine benthic $\delta^{18}O$ records: Reviews of Geophysics, v. 52, p. 333–374.

NEBELSICK, J.H. and BASSI, D., 2000, Diversity, growth-forms and taphonomy: key factors controlling the fabric of coralline algal dominated shelf carbonates, *in* E. Insalaco, P.W. Skelton, and T.J. Palmer (eds.), Carbonate Platform Systems: Components and Interactions: Geological Society Special Publications, v. 178, 89–107.

NEBELSICK, J.H., BASSI, D., and RASSER, M.W., 2011, Microtaphofacies: exploring the potential for taphonomic analysis in carbonates, *in* P. Allison and D.J. Bottjer (eds.), Taphonomy: Process and Bias Through Time: Topics in Geobiology: Springer Science + Business, Dordrecht, Heidelberg, London, New York, v. 32, 337–377.

NITSCH, F., NEBELSICK, J.H., and BASSI, D., 2015, Constructional and destructional patterns—void classification of rhodoliths from Giglio Island: PALAIOS, v. 30, p. 380–691.

ÖZCAN, E., LESS, G., BÁLDI-BEKE, M., KOLLÁNYI, K., and ACAR, F., 2009, Oligo-Miocene foraminiferal record (Miogypsinidae, Lepidocyclinidae and Nummulitidae) from the Western Taurides (SW Turkey): biometry and implications for the regional geology: Journal of Asian Earth Sciences, v. 287, p. 20–38.

ÖZCAN, E., LESS, GY., BÁLDI-BEKE, M., and KOLLÁNYI K., 2010, Oligocene hyaline larger foraminifera from Kelereşdere Section (Muş, Eastern Turkey): Micropaleontology, v. 56, p. 465–493.

PARENTE, M., 1994, A revised stratigraphy of the Upper Cretaceous to Oligocene units from southeastern Salento (Apulia, southern Italy): Bollettino della Società Paleontologica Italiana, v. 33, p. 155–170.

POMAR, L., MATEU-VICENS, G., MORSILLI, M., and BRANDANO, M., 2014, Carbonate ramp evolution during the late Oligocene (Chattian), Salento Peninsula, southern Italy: Palaeogeography, Palaeoclimatology, Palaeoecology, v. 404, p. 109–132.

POMAR, L., ESTEBAN, M., MARTINEZ, W., ESPINO, D., CASTILLO DE OTT, V., BENKOVICS, L., and CASTRO LEYVA, T., 2015, Oligocene–Miocene carbonates of the Perla Field, Offshore Venezuela: Depositional model and facies architecture: AAPG Special Publication, v. 108, p. 647–674.

POPESCU, G. and CRIHAN, I.M., 2008, Contributions to the knowledge of the rotaliiform foraminifera from marine middle Miocene deposits from Romania: Acta Palaeontologica Romaniae, v. 6, p. 287–324.

REUTER, M., PILLER, W.E., BRANDANO, M., and HARZHAUSER, M., 2013, Correlating Mediterranean shallow water deposits with global Oligocene–Miocene stratigraphy and oceanic events: Global and Planetary Change, v. 111, p. 226–236.

REUTER, M., PILLER, W.E., HARZHAUSER, M., MANDIC, O., BERNING, B., RÖGL, F., KROH, A., AUBRY, M.-P., WIELANDT-SCHUSTER, U., and HAMEDANI, A., 2009, The Oligo-/Miocene Qom Formation (Iran): evidence for an early Burdigalian restriction of the Tethyan Seaway and closure of its Iranian gateways: International Journal of Earth Sciences, v. 98, p. 627–650.

ROBINSON, E., 1995, Larger foraminiferal assemblages from Oligocene platform carbonates, Jamaica: Tethyan or Caribbean?: Marine Micropaleontology, v. 26, p. 313–318.
ROCA, E., 1992, L'estructura de la conca Catalano-Balear: paper de la compressió i de la distensió en la seva gènesi: Ph.D. thesis, University of Barcelona, 330 p.
RÖGL, F. and BRANDSTÄTTER, F., 1993, The foraminifera genus *Amphistegina* in the Korytriica Clays (Holy Cross Mts, Central Poland) and its significance in the Miocene of the Paratethys Acta Geologica Polonica, v. 43, no. 1–2, p. 121–146.
ROMERO, J., CAUS, E., and ROSELL, J., 2002, A model for the palaeoenvironmental distribution of larger foraminifera based on late middle Eocene deposits on the margin of the South Pyrenean basin (NE Spain): Palaeogeography, Palaeoclimatology, Palaeoecology, v. 179, p. 43–56.
SADEGHI, R., VAZIRI-MOGHADDAM, H., and TAHERI, A., 2011, Microfacies and sedimentary environment of the Oligocene sequence (Asmari Formation) in Fars sub-basin, Zagros Mountains, southwest Iran: Facies, v. 57, p. 431–446.
SCHIAVINOTTO, F. and VERRUBBI, V., 1994, *Nephrolepidina* in the Oligo-Miocene section of the Gran Sasso (Central Apennines): environment-evolution relations: Bollettino della Società Paleontologica Italiana, v. 33, p. 375–406.
SHABAFROOZ, R., MAHBOUBI, A., VAZIRI-MOGHADDAM, H., GHABEISHAVI, A., and MOUSSAVI-HARAMI, R., 2015, Depositional architecture and sequence stratigraphy of the Oligo-Miocene Asmari platform; Southeastern Izeh Zone, Zagros Basin, Iran: Facies, v. 61, p. 423.
SHARAF, E., SIMO, J.A., CARROLL, A.R., and SHIELDS, M., 2005, Stratigraphic evolution of Oligocene–Miocene carbonates and siliciclastics, East Java basin, Indonesia: AAPG Bulletin, v. 89, p. 799–819.
SILVESTRI, G., BOSELLINI, F.R., and NEBELSICK, J.H., 2011, Microtaphofacies analysis of lower Oligocene turbid-water coral assemblages: PALAIOS, v. 26, p. 805–820.
STOKLOSA, M. and SIMO, J.A., 2008, Tectonic controls on Oligocene carbonate platform-basin deposition, Costa Blanca, southeast Spain, *in* J. Lukasik and J.A. Simo (eds.), Controls on Carbonate Platform and Reef Development: SEPM Special Publication, v. 89, p. 171–184.
VAN BUCHEM, F.S.P., ALLAN, T.L., LAURSEN, G.V., LOTFPOUR, M., MOALLEMI, A., MONIBI, S., MOTIEI, H., PICKARD, N.A.H., TAHMASBI, A.R., VEDRENNE, V., and VINCENT, B., 2010, Regional stratigraphic architecture and reservoir types of the Oligo-Miocene deposits in the Dezful Embayment (Asmari and Pabdeh Formations) SW Iran: Geological Society, London, Special Publications, v. 329, p. 219–263.
VAZIRI-MOGHADDAM, H., KIMIAGARI, M., and TAHERI, A., 2006, Depositional environment and sequence stratigraphy of the Oligo-Miocene Asmari Formation in SW Iran: Facies, v. 52, p. 41–51.
VEGAS, R., PEDRAZA, J., CABAÑAS, I., and URALDE, M.A., 1973, Jávea, hoja n° 823, mapa geológico de España 1:50.000: Servicio de Publicaciones, Ministerio de Industria, Madrid, 2ª Serie. 1ª Edición, 15 p.
VERA, J.A., 2000, El Terciario de la Cordillera Bética: estado actual de conocimientos: Revista de la Sociedad Geológica de España, v. 13, p. 345–373.
WHEELER, C.B., 1963, Oligocene and lower Miocene stratigraphy of western and northeastern Falcón Basin, Venezuela: AAPG Bulletin, v. 47, p. 35–68.

WIGLEY, R. and COMPTON, J.S., 2007, Oligocene to Holocene glauconite-phosphorite grains from the Head of the Cape Canyon on the western margin of South Africa: Deep-ea Research, v. 54, p. 1375–1395.
ZACHOS, J., PAGANI, M., SLOAN, L., THOMAS, E. and BILLUPS, K., 2001, Trends, rhythms, and aberrations in global climate 65 Ma to present: Science, v. 292, p. 686–693.
ZALASIEWICZ, J., SMITH, A., BRENCHLEY, P., EVANS, J., KNOX, R., RILEY, N., GALE, A., GREGORY, F.J., RUSHTON, A., GIBBARD, P., HESSELBO, S., MARSHALL, J., OATES, M., RAWSON, P., and TREWIN, N., 2004, Simplifying the stratigraphy of time: Geology, v. 32, p. 1–4.
Received 20 January 2016; accepted 26 May 2016.
Figure Captions:
FIG. 1.—Geographical and paleogeographical setting. **A**) Geological map of the study area showing Cretaceous, Oligocene, Miocene and Quaternary lithological units (modified from Vegas et al. 1973). The white and red stars indicate the location of the outcrops investigated: 1, Torre Garcia-Cim del Sol Road section (Rupelian?–early Miocene); 2, Accés Sud Road section (Chattian–early Miocene); 3, Albacete Road section (Chattian–early Miocene); 4, Rebaldí section (Cretaceous and Chattian). Inset: the situation of the Prebetic Zone, the Betic Cordillera and the outcrops studied in the southeastern Iberian Peninsula. **B**) Paleogeographic reconstruction of the Tethys during the early Chattian (~ 28 Ma) (after Dercourt et al. 2000 and Knoerich and Mutti 2003). The situation of the Prebetic Domain is marked with a white and red star.
FIG. 2.—Stratigraphic setting. **A**) Panoramic view of the Benitatxell Range showing the stratigraphic situation of the Cretaceous substrate and the studied Chattian coralline algal limestones with lepidocyclinids. Width of image is approximately 1.85 km. **B**) Outcrop view of the Torre Garcia-Cim del Sol Road section. The unconformity between the Cretaceous substrate and the Oligocene sedimentary succession, as well as the situation of the Chattian coralline algal limestone beds with lepidocyclinids examined, are indicated. Width of image is approximately 400 m. **C**) Outcrop photograph of the Oligocene succession made up of marl and limestone with echinoids and planktonic foraminifera underlying the lepidocyclinid-bearing beds studied. Torre Garcia-Cim del Sol Road section. Hammer = 32 cm.
FIG. 3.—Outcrop-scale photographs of the sedimentary successions studied. **A**) View of the Chattian coralline algal limestones with lepidocyclinids in the Torre Garcia-Cim del Sol Road section. Width of image is approximately 120 m. **B**) Detail of the Chattian strata analyzed along the Accés Sud Road section. Width of image is around 4 m. **C**) View of the Chattian lepidocyclinid and coralline algal limestone exposed along the Albacete Road section. Jacob's staff = 1.5 m. **D**) Image of the Chattian platform carbonates exposed in the Rebaldí section. Prograding clinoforms are highlighted with a white discontinuous line. The stratigraphic position of the identified *Microcodium* structures is indicated. The carbonate succession is 9 m thick. **E**) View of the subaerial unconformity between the Cretaceous white wackestone with planktic foraminifera (below) and the Chattian platform carbonates with coralline algae and benthic foraminifera (above). Rebaldí section. Hammer = 32 cm. **F**) Marls and silty to sandy limestones rich in planktonic foraminifera and glauconite of early Miocene age overlying the Chattian carbonates with coralline algae and benthic foraminifera investigated in the Torre Garcia-Cim del Sol Road section. Hammer = 32 cm.
FIG. 4.—Stratigraphic log of the Torre Garcia-Cim del Sol Road section showing textures, sedimentary structures and qualitative abundances of skeletal and non-skeletal

components, as well as of biostratinomic signatures. See Figures 1A and 5 for location of the profile and key, respectively.

FIG. 5.—Stratigraphic logs. **A**) Accés Sud Road section. **B**) Albacete Road section. Textures, sedimentary structures, and qualitative abundances of skeletal and non-skeletal components, are shown as well as biostratinomic signatures. See Figure 1A for location of the sections.

FIG. 6.—Stratigraphic log of the Rebaldí section showing textures, sedimentary structures and qualitative abundances of skeletal and non-skeletal components, as well as biostratinomic signatures. See Figures 1A and 5 for location of the section and key, respectively.

FIG. 7.—Outcrop images and thin-section photomicrographs of representative Chattian biotic composition and facies from the Benitatxell Range. **A**) Detail of a rudstone texture dominated by lepidocyclinids. The conspicuous larger specimens correspond to *Eulepidina elephantina*. Accés Sud Road section. Coin diameter = 1.625 cm. **B**) Photomicrograph of a rudstone texture with the lepidocyclinid *Nephrolepidina* sp. occurring in rock-forming abundance. Meter 3 in the Albacete Road section. Scale bar = 0.5 mm. **C**) Bedding plane of a coarse rudstone texture with well-preserved pectinids. This surface corresponds to the top of the Chattian limestone with benthic foraminifera and coralline algae in the Torre Garcia-Cim del Sol Road section. Scale bar = 4 cm. **D**) Detail of a spheroidal rhodolith from Torre Garcia-Cim del Sol Road section. Pen = 3.6 cm.

FIG. 8.—Representative Chattian coralline algae from the Torre Garcia-Cim del Sol Road section (Benitatxell Range). **A**) *Lithothmanion ramosissimum* showing empty multiporate sporangial conceptacles. **B**) Encrusting *Mesophyllum* sp. 1 growing on micrite-rich carbonate. **C**) Branch of *Sporolithon lugeonii* showing buried isolated sporangial cavities grouped in a sorus. **D**) Encrusting *Spongites* sp. 1 with several uniporate sporangial conceptacles. **E**) Fruticose growth of *Spongites* sp. 2 characterized by trapezoidal uniporate sporangial conceptacles. **F**) Encrusting *Neogoniolithon contii* with a large uniporate sporangial conceptacle. Yellow arrow points to the pore canal in a marginal section.

FIG. 9.—Representative Chattian benthic foraminifera from the Benitatxell Range identified at species level. **A**) *Miogypsinoides formosensis*. Accés Sud Road section. **B**) *Eulepidina dilatata*. Accés Sud Road section. **C**) *Eulepidina elephantina*. Torre Garcia-Cim del Sol Road section. **D**) *Heterostegina assilinoides*. Torre Garcia-Cim del Sol Road section. **E**) *Spiroclypeus blanckenhorni*. Accés Sud Road section. **F**) *Risananeiza pustulosa*. Torre Garcia-Cim del Sol Road section. **G**) *Neorotalia viennoti*. Torre Garcia-Cim del Sol Road section.

FIG. 10.—Microtaphofacies from the Benitatxell Range. **A**) Photomicrograph showing a coral fragment (c) encrusted by a multi-taxon sequence including different coralline algal species (ca), and bryozoans (b). Note the presence of *Amphistegina* (a) and *Risananeiza pustulosa* (r) at the lower left corner. Torre Garcia-Cim del Sol Road section. Scale bar = 1 mm. **B**) Pervasively bioeroded test of *Eulepidina elephantina* (e). Note the presence of geopetal infillings within the boring structures, and of *Amphistegina bohdanowiczi* (a) at the lower right part of the image. Accés Sud Road section. Scale bar = 1 mm. **C**) Photomicrograph of highly fragmented skeletal components. Note the presence of a damaged test of *Nephrolepidina* sp. (n) at the center of the image. Torre Garcia-Cim del Sol Road section. Scale bar = 1 mm. **D**) Photomicrograph of abraded tests of *Neorotalia viennoti* (ne), *Nummulites* cf. *vascus* (nu), *Nephrolepidina* sp. (n) and *Eulepidina elephantina* (e), which is encrusted by

coralline algae (ca) (yellow arrows). Torre Garcia-Cim del Sol Road section. Scale bar = 1 mm.

FIG. 11.—Outcrop images and thin-section photomicrographs of representative late Chattian biotic components and facies from the Rebaldí section. **A**) Representative photomicrograph of the microfacies giving rise to the platform carbonates of the Rebaldí section. Common skeletal components include *Risananeiza* sp. (r), fragments of coralline algae (ca), *Amphistegina bohdanowiczi* (a), *Heterostegina* sp. (h), miliolids (m), *Miogypsinoides complanatus* (mi), textularids (t) and *Nephrolepidina* sp. (n). Scale bar = 1 mm. **B**) Photograph of a branching coral colony preserved in growth position. Camera cap = 5.8 cm. **C**) Detail view of a fragment of a dasycladacean alga (yellow arrow). Scale bar = 1 mm. **D**) Detail view of pervasive *Paronipora* (=*Microcodium*) on a scleractinian coral. Scale bar = 1 mm.

FIG. 12.—Representative Chattian coralline algae from the Rebaldí section. **A**) *Sporolithon* sp. 1 showing a sorus consisting of a few isolated calcified sporangial chambers. A large, trapezoidal stalk cell is preserved at the base of one of the chambers. Scale bar = 100 µm. **B**) Fragmented and abraded branches of *Lithothamnion* sp. 1 with numerous large multiporate sporangial conceptacles. Scale bar = 200 µm. **C**) Branch of *Lithothamnion* sp. 3. This species is characterized by a consistently zonated thallus preserving a few buried small ovate multiporate sporangial conceptacles. Scale bar = 200 µm. **D**) Laminar thallus of *Mesophyllum* sp. 2. Two pores are clearly visible in the roof of the sporangial conceptacle chamber. Scale bar = 200 µm. **E**) Thin, laminar coralline algal thalli with dimerous organization. Scale bar = 200 µm. **F**) Articulated geniculate coralline alga. Scale bar = 100 µm. **G**) *Polystrata alba*. Note the miliolid at the upper part of the image. Scale bar = 100 µm.

FIG. 13.—Representative Chattian benthic foraminifera from the Rebaldí section determined at genus and species levels. **A**) *Planorbulina* sp. Scale bar = 100 µm. **B**) *Planorbulinella* sp. Scale bar = 100 µm. **C**) *Peneroplis thomasi*. Scale bar = 100 µm. **D**) *Austrotrillina asmariensis*. Scale bar = 200 µm. **E**) *Amphistegina bohdanowiczi*. Scale bar = 200 µm. **F**) *Neorotalia lithothamnica*. Scale bar = 200 µm. **G**) *Miogypsinoides complanatus*. Scale bar = 500 µm. **H**) *Sphaerogypsina* sp. Scale bar = 500 µm. **I**) *Spiroclypeus blanckenhorni*. Scale bar = 500 µm. **J**) *Risananeiza pustulosa*. Scale bar = 500 µm. **K**) *Heterostegina* aff. *assilinoides*. Scale bar = 500 µm. **L**) *Carpenteria* sp. Scale bar = 500 µm. **M**) *Haddonia heissigi*. Scale bar = 500 µm.

FIG. 14.—Correlation of the stratigraphic columns logged in Rebaldí and the Benitatxell Range showing distribution of main components, facies and the sequence-stratigraphic analysis. See Figure 1A for location of the stratigraphic logs and Figures 4–6 for textures and detailed distribution and qualitative abundances of skeletal and non-skeletal constituents.

FIG. 15.—Schematic depositional model resulting from the application of Walter's Law showing the lateral facies relationships and biotic occurrences for the late and latest Chattian carbonates studied in Rebaldí and the Benitatxell Range. Note the homoclinal ramp depositional profile interpreted for the Rebaldí-Benitatxell Range carbonate system. Biogenic components are represented roughly in their original habitats from shallower to deeper ramp settings, following Hallock and Glenn (1986), Buxton (1988), Schiavinotto and Verrubbi (1994), Hottinger (1997), Geel (2000), Romero et al. (2002), Beavington-Penney and Racey (2004), Brandano et al. (2009b, 2012), Bassi and Nebelsick (2010), van Buchem et al. (2010), Pomar et al. (2014) and Brandano (2016).

FIG. 16.—Conceptual model for the sedimentary evolution of the late Chattian carbonate system analyzed in Rebaldí and the Benitatxell Range in relation to changes of relative sea level. The model is based on the sequence-stratigraphic analysis shown in

Figure 14. See this latter figure for key. **A**) Sedimentary architecture generated above the Cretaceous substrate during the Rupelian?–late Chattian transgressive and early regressive stages of Sequence I. **B**) Latest Chattian deposition of platform carbonates and marls and limestones with echinoids and planktic foraminifera during the late regressive stage of Sequence I and the early transgressive stage of Sequence II. During the late regressive stage of Sequence I, the proximal ramp was subaerially exposed and *Microcodium* structures developed on top of this regressive unit. **C**) Drowning of the latest Chattian lepidocyclinid-bearing carbonate platform and deposition of marls and silty to sandy limestones with planktonic foraminifera and glauconite during a later transgressive stage of Sequence II.

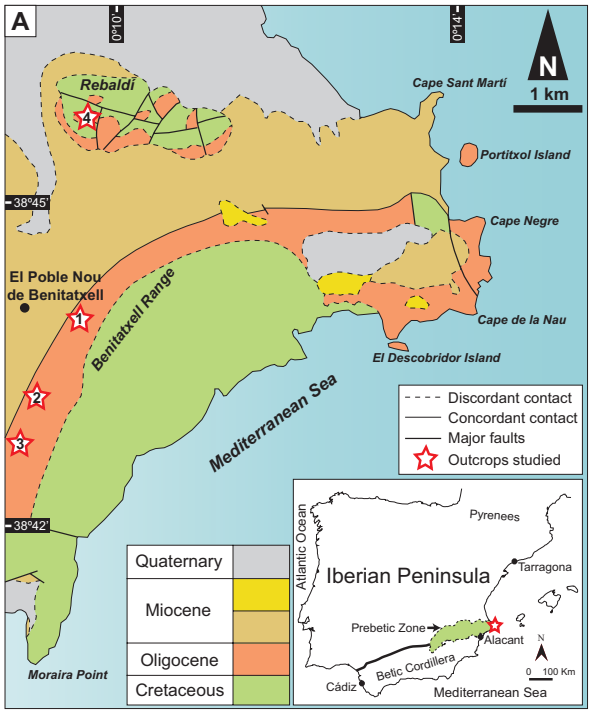
A
0°10'
0°14'
N
1 km
Rebaldi
Cape Sant Martí
Portitxol Island
38°45'
Cape Negre
El Poble Nou
de Benitatxell
Benitatxell Range
Cape de la Nau
El Descobridor Island
Mediterranean Sea
Discordant contact
Concordant contact
Major faults
Outcrops studied
38°42'
Quaternary
Miocene
Oligocene
Cretaceous
Moraira Point
Atlantic Ocean
Pyrenees
Iberian Peninsula
Tarragona
Prebetic Zone
Alacant
Betic Cordillera
Cádiz
Mediterranean Sea
0 100 Km

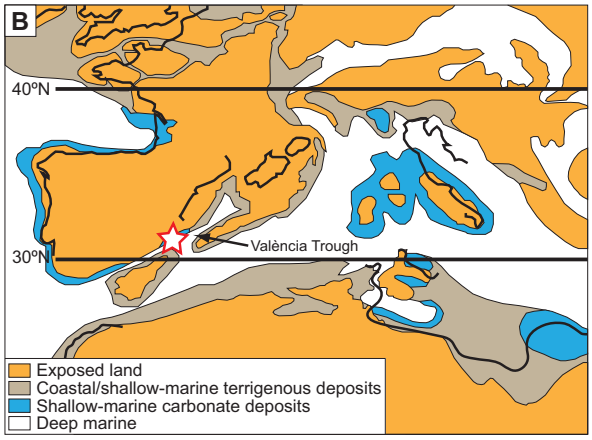
B
40ºN
30ºN
València Trough
Exposed land
Coastal/shallow-marine terrigenous deposits
Shallow-marine carbonate deposits
Deep marine

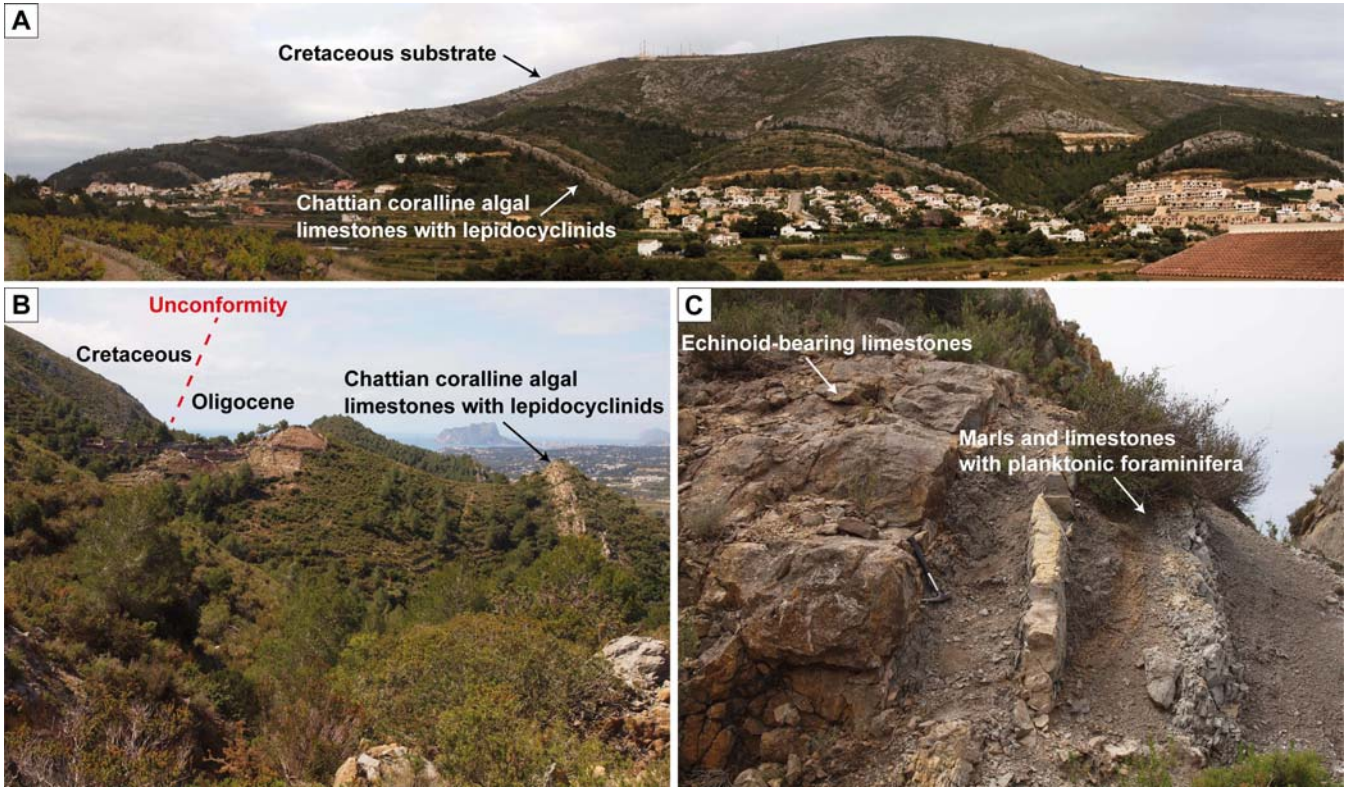
A
Cretaceous substrate
Chattian coralline algal
limestones with lepidocyclinids
B
Unconformity
Cretaceous
Oligocene
Chattian coralline algal
limestones with lepidocyclinids
C
Echinoid-bearing limestones
Marls and limestones
with planktonic foraminifera


A
B
C
D
Microcodium
prograding
downlapping
E
late Chattian
Unconformity
Cretaceous
F

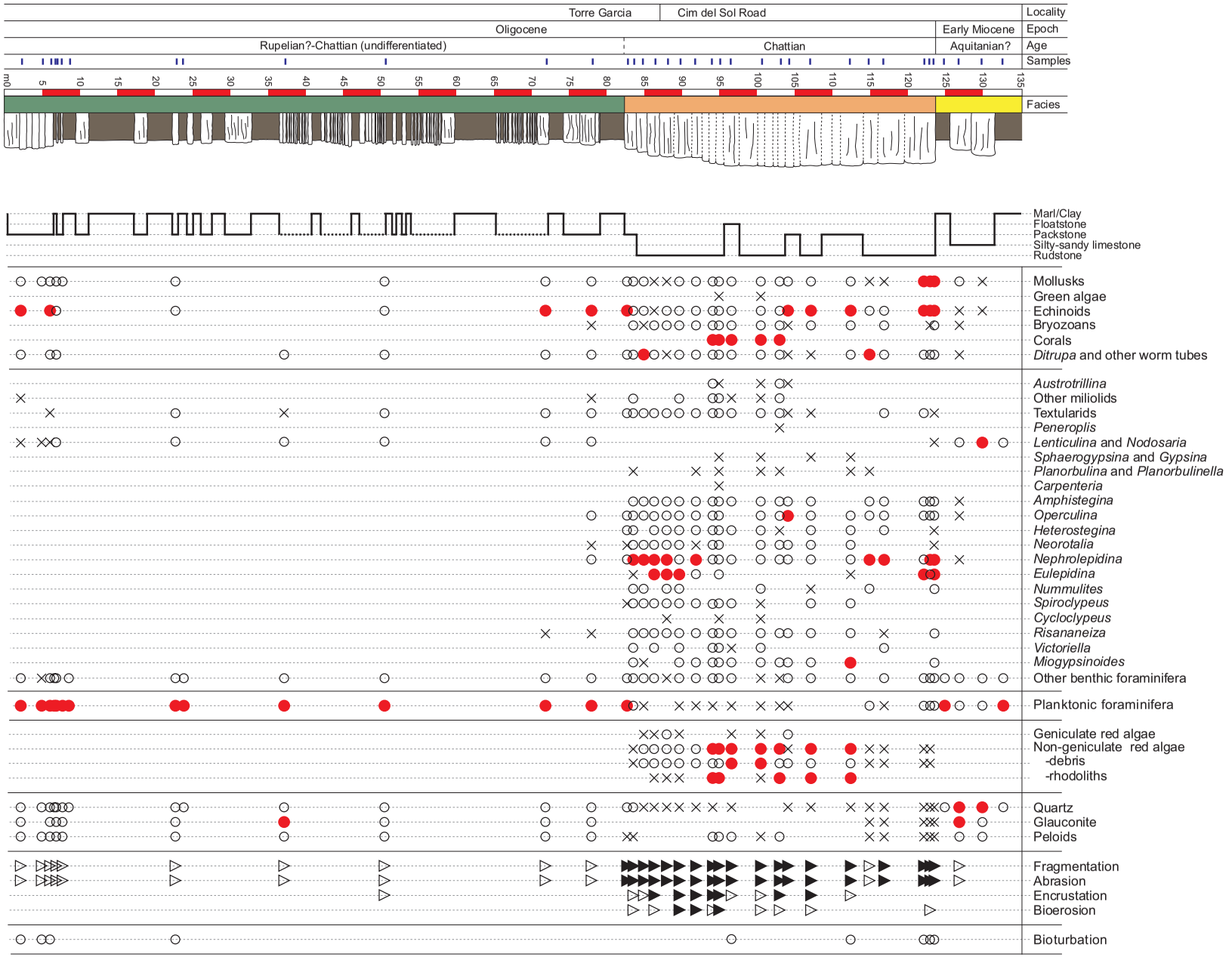
Torre Garcia
Cim del Sol Road
Locality
Oligocene
Early Miocene
Epoch
Rupelian?-Chattian (undifferentiated)
Chattian
Aquitanian?
Age
Samples
m0
5
10
15
20
25
30
35
40
45
50
55
60
65
70
75
80
85
90
95
100
105
110
115
120
125
130
135
Facies
Marl/Clay
Floatstone
Packstone
Silty-sandy limestone
Rudstone
Mollusks
Green algae
Echinoids
Bryozoans
Corals
Ditrupa and other worm tubes
Austrotrillina
Other miliolids
Textularids
Peneroplis
Lenticulina and Nodosaria
Sphaerogypsina and Gypsina
Planorbulina and Planorbulinella
Carpenteria
Amphistegina
Operculina
Heterostegina
Neorotalia
Nephrolepidina
Eulepidina
Nummulites
Spiroclypeus
Cycloclypeus
Risananeiza
Victoriella
Miogypsinoides
Other benthic foraminifera
Planktonic foraminifera
Geniculate red algae
Non-geniculate red algae
-debris
-rhodoliths
Quartz
Glauconite
Peloids
Fragmentation
Abrasion
Encrustation
Bioerosion
Bioturbation

A
Accès Sud Road
Locality
Epoch
Age
Samples
Facies
Oligocene
Miocene
Chattian
Aquitan.?
m0
5
10
15
20
25
27
Marl/Clay
Floatstone
Packstone
Silty-sandy limestone
Rudstone
Mollusks
Green algae
Echinoids
Bryozoans
Corals
Ditrupa and other worm tubes
Austrotrillina
Other miliolids
Textularids
Peneroplis
Lenticulina and Nodosaria
Sphaerogypsina and Gypsina
Planorbulina and Planorbulinella
Carpenteria
Amphistegina
Operculina
Heterostegina
Neorotalia
Nephrolepidina
Eulepidina
Nummulites
Spiroclypeus
Cycloclypeus
Risananeiza
Miogypsinoides
Other benthic foraminifera
Planktonic foraminifera
Geniculate red algae
Non-geniculate red algae
-debris
-rhodoliths
Quartz
Glauconite
Peloids
Fragmentation
Abrasion
Encrustation
Bioerosion
Bioturbation
B
Albacete Road
Aquita.?
32
30
25
20
15
Victoriella
Key
High
Low
Lack of evident stratification
Marl
Limestone
Marls and silty-sandy limestones with planktonic foraminifera and glauconite
Limestones with benthic foraminifera and coralline algae
Marls and limestones with echinoids and planktonic foraminifera
Well-bedded white limestones with planktonic foraminifera
Facies-characteristic component
Common component or bioturbation structures
Rare component

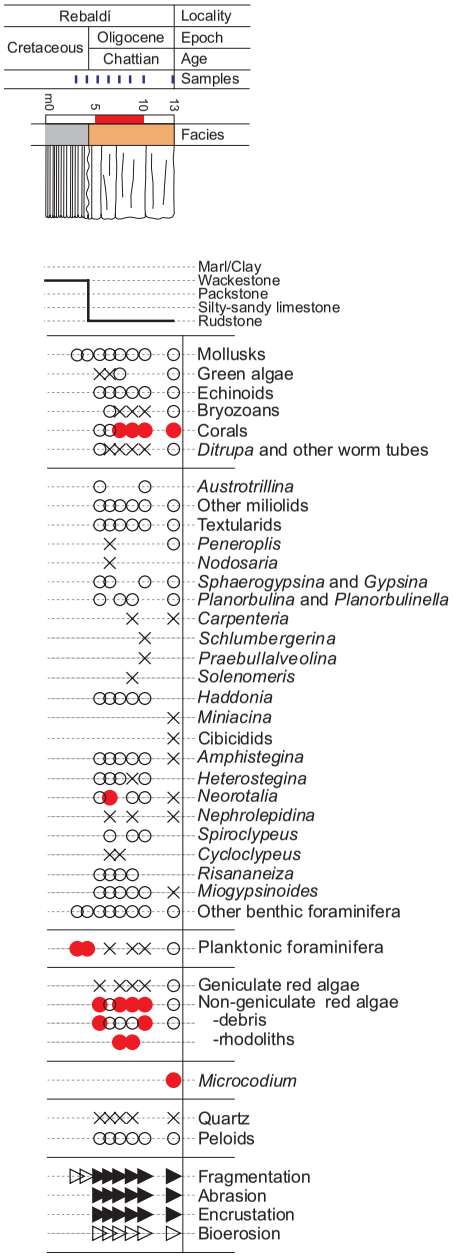
Rebaldí
Locality
Cretaceous
Oligocene
Epoch
Chattian
Age
Samples
m0
5
10
13
Facies
Marl/Clay
Wackestone
Packstone
Silty-sandy limestone
Rudstone
Mollusks
Green algae
Echinoids
Bryozoans
Corals
Ditrupa and other worm tubes
Austrotrillina
Other miliolids
Textularids
Peneroplis
Nodosaria
Sphaerogypsina and Gypsina
Planorbulina and Planorbulinella
Carpenteria
Schlumbergerina
Praebullalveolina
Solenomeris
Haddonia
Miniacina
Cibicidids
Amphistegina
Heterostegina
Neorotalia
Nephrolepidina
Spiroclypeus
Cycloclypeus
Risananeiza
Miogypsinoides
Other benthic foraminifera
Planktonic foraminifera
Geniculate red algae
Non-geniculate red algae
-debris
-rhodoliths
Microcodium
Quartz
Peloids
Fragmentation
Abrasion
Encrustation
Bioerosion

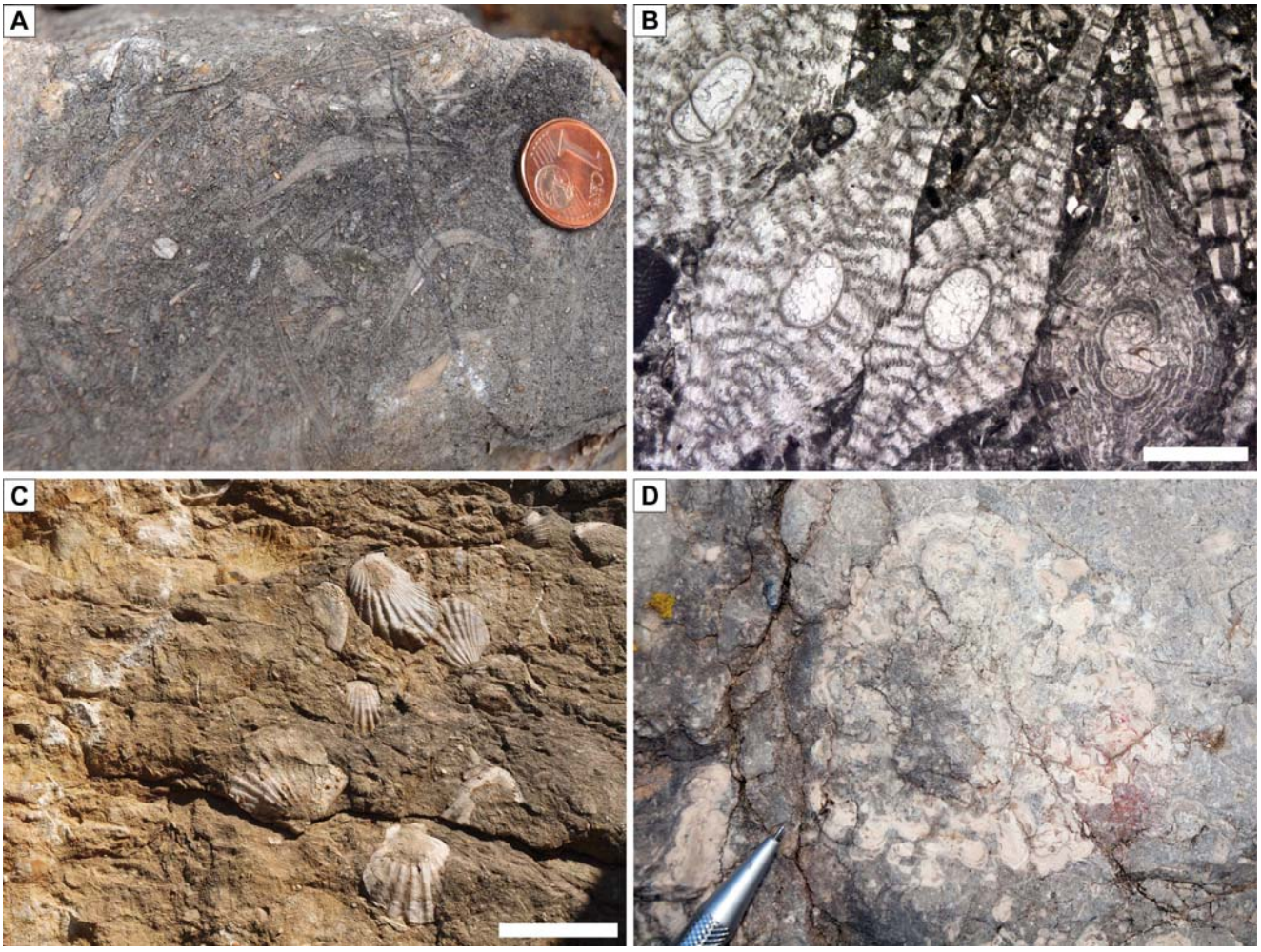
A
B
C
D

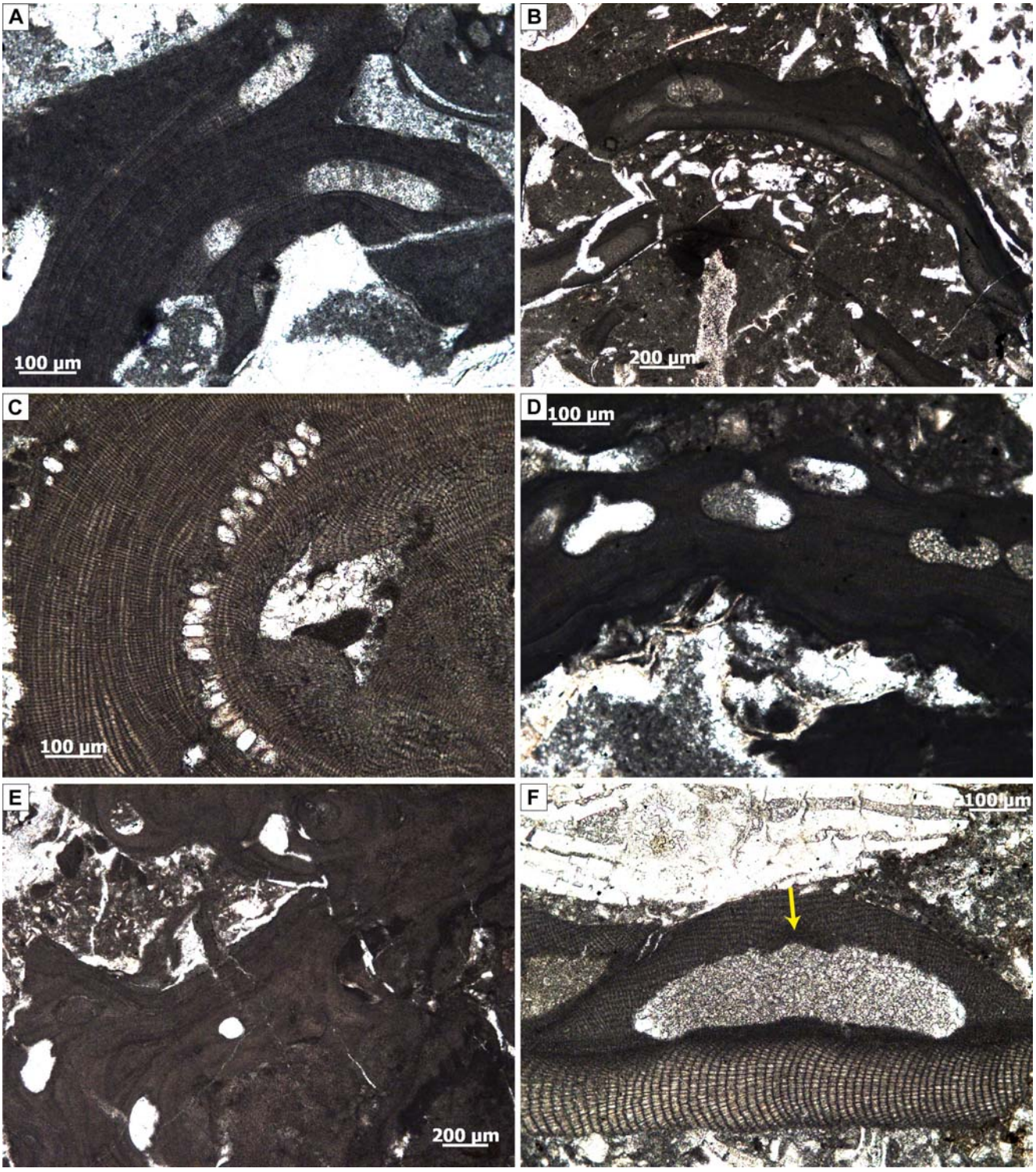
A
100 µm
B
200 µm
C
100 µm
D
100 µm
E
200 µm
F
100 µm

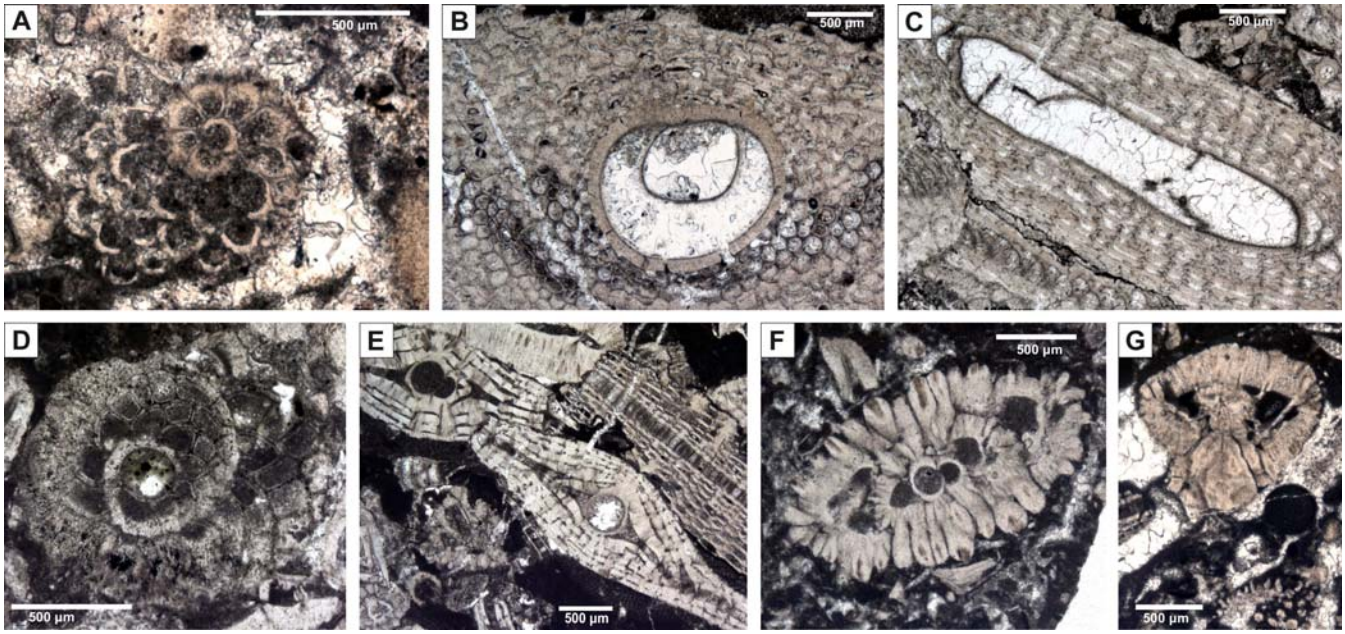
A
500 µm
B
500 µm
C
500 µm
D
500 µm
E
500 µm
F
500 µm
G
500 µm

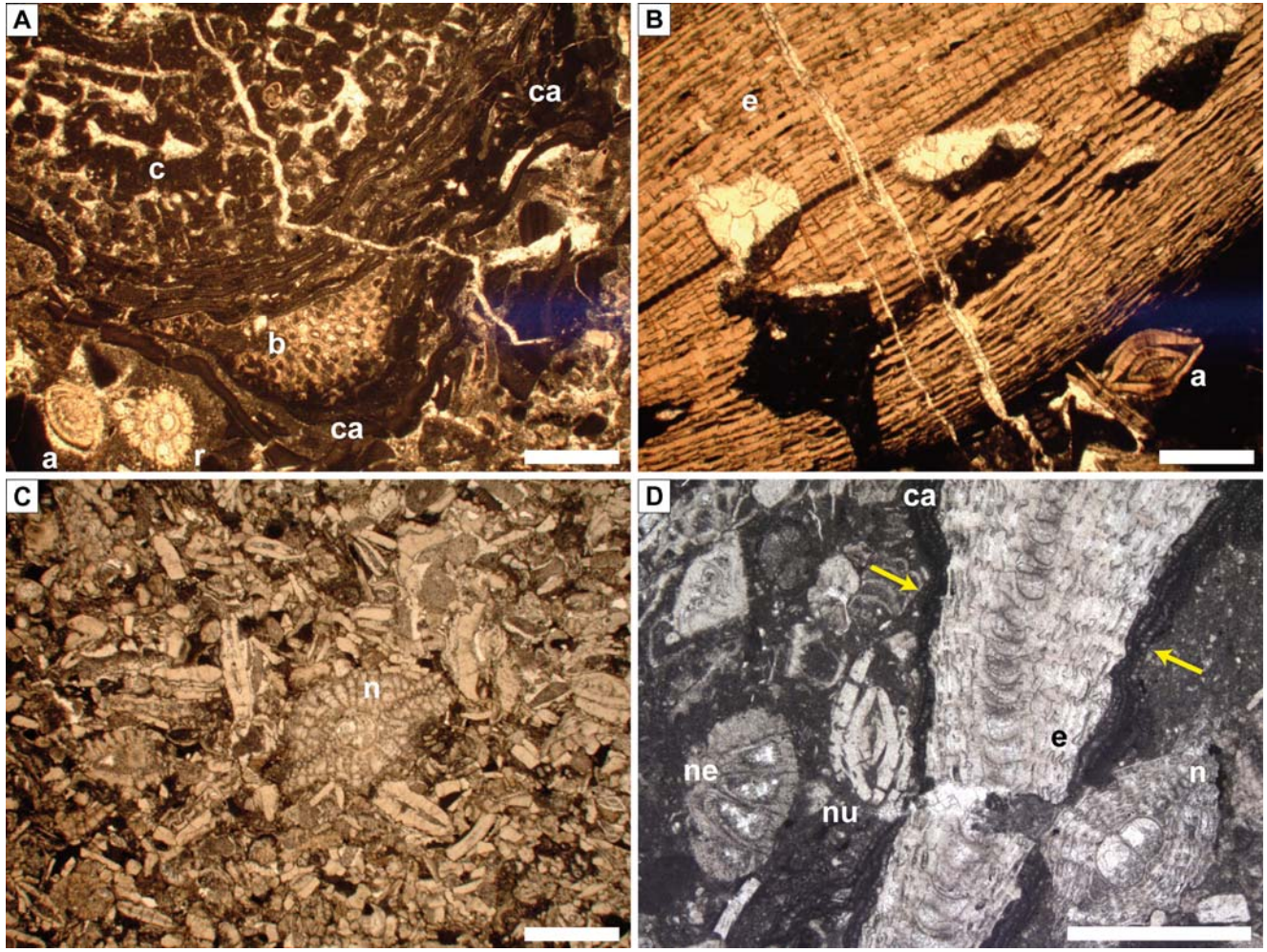
A
ca
c
b
ca
a
r
B
e
a
C
n
D
ca
e
ne
nu
n

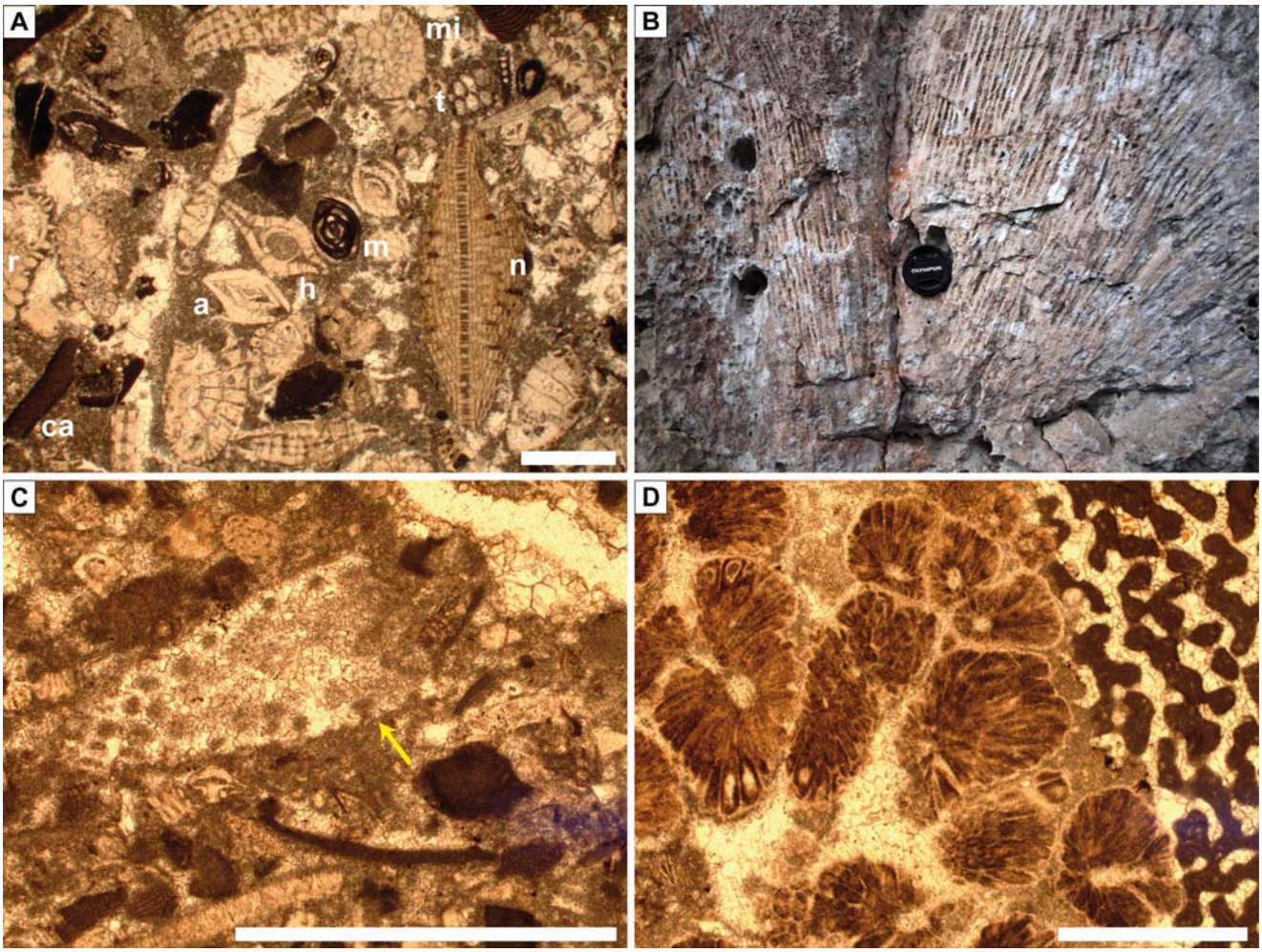
A
mi
t
r
m
n
h
a
ca
B
C
D

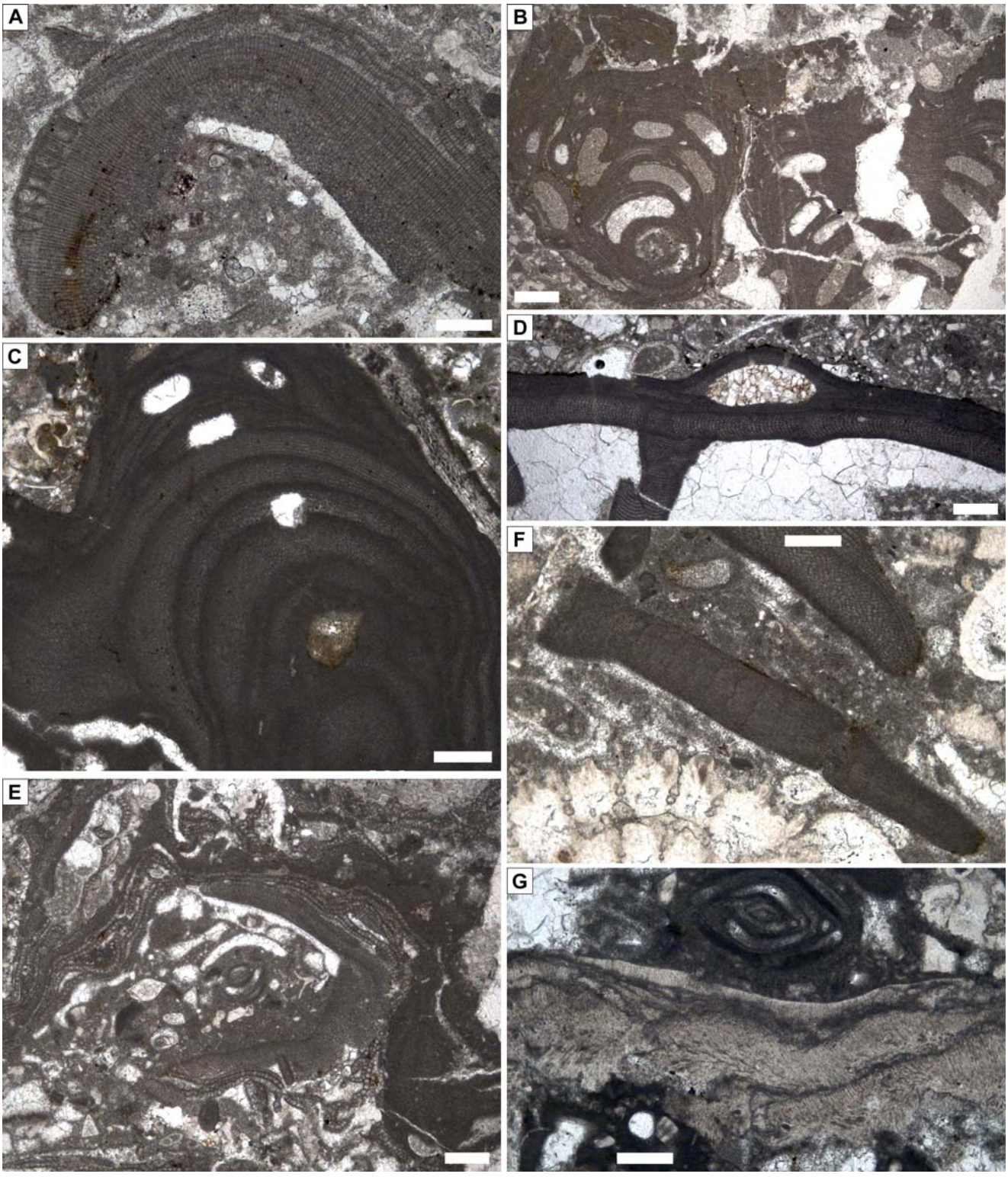
A
B
C
D
E
F
G

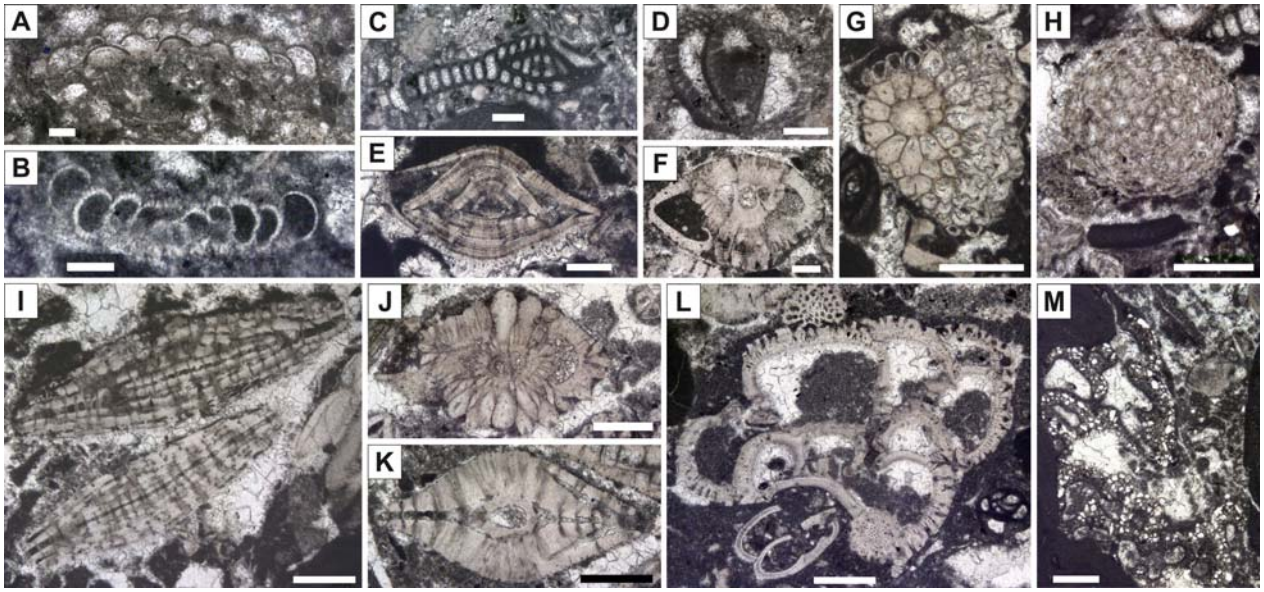
A
B
C
E
D
F
G
H
I
J
K
L
M

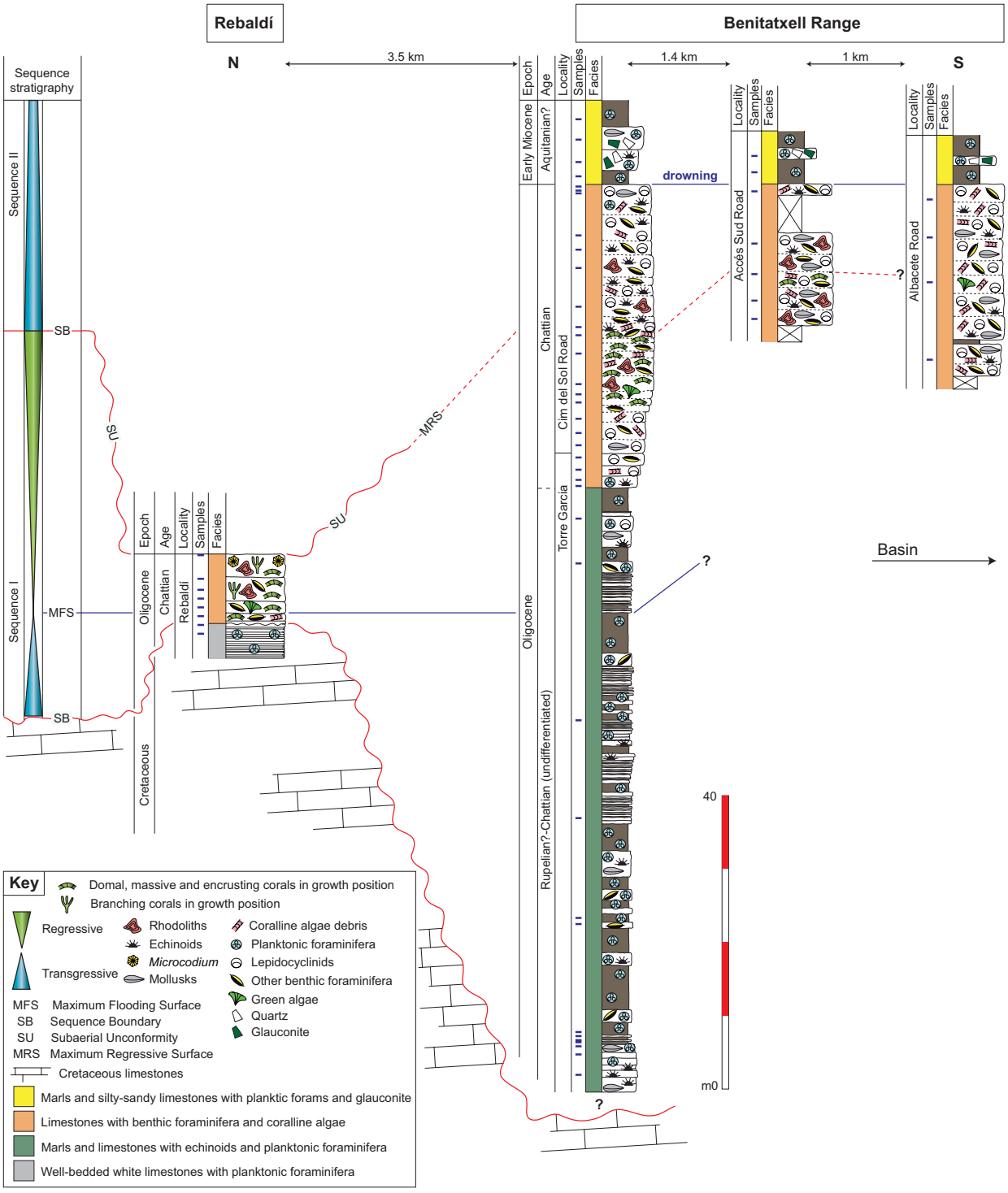
Rebaldí
Benitatxell Range
N
S
3.5 km
1.4 km
1 km
Basin
Sequence stratigraphy
Sequence II
Sequence I
SB
MFS
SB
SU
SU
MRS
Epoch
Age
Locality
Samples
Facies
Oligocene
Chattian
Rebaldí
Cretaceous
Early Miocene
Aquitanian?
Oligocene
Chattian
Cim del Sol Road
Torre Garcia
Rupelian?-Chattian (undifferentiated)
drowning
Accés Sud Road
Albacete Road
?
?
?
40
m0
Key
Domal, massive and encrusting corals in growth position
Branching corals in growth position
Regressive
Transgressive
Rhodoliths
Echinoids
Microcodium
Mollusks
Coralline algae debris
Planktonic foraminifera
Lepidocyclinids
Other benthic foraminifera
Green algae
Quartz
Glauconite
MFS Maximum Flooding Surface
SB Sequence Boundary
SU Subaerial Unconformity
MRS Maximum Regressive Surface
Cretaceous limestones
Marls and silty-sandy limestones with planktic forams and glauconite
Limestones with benthic foraminifera and coralline algae
Marls and limestones with echinoids and planktonic foraminifera
Well-bedded white limestones with planktonic foraminifera

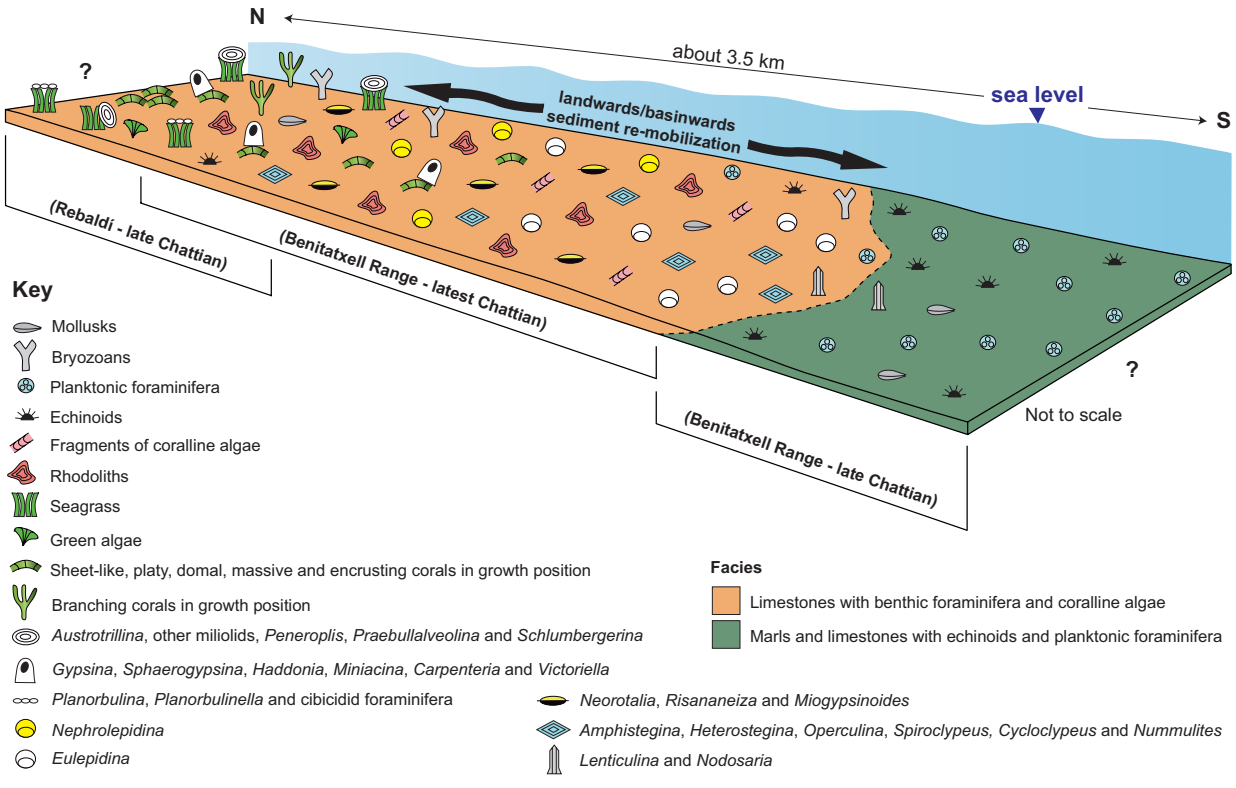
N
about 3.5 km
sea level
S
?
landwards/basinwards
sediment re-mobilization
(Rebaldi - late Chattian)
(Benitatxell Range - latest Chattian)
(Benitatxell Range - late Chattian)
?
Not to scale
Key
Mollusks
Bryozoans
Planktonic foraminifera
Echinoids
Fragments of coralline algae
Rhodoliths
Seagrass
Green algae
Sheet-like, platy, domal, massive and encrusting corals in growth position
Branching corals in growth position
Austrotrillina, other miliolids, Peneroplis, Praebullalveolina and Schlumbergerina
Gypsina, Sphaerogypsina, Haddonia, Miniacina, Carpenteria and Victoriella
Planorbulina, Planorbulinella and cibicidid foraminifera
Nephrolepidina
Eulepidina
Neorotalia, Risananeiza and Miogypsinoides
Amphistegina, Heterostegina, Operculina, Spiroclypeus, Cycloclypeus and Nummulites
Lenticulina and Nodosaria
Facies
Limestones with benthic foraminifera and coralline algae
Marls and limestones with echinoids and planktonic foraminifera

C Later transgressive stage of Sequence II (early Miocene)

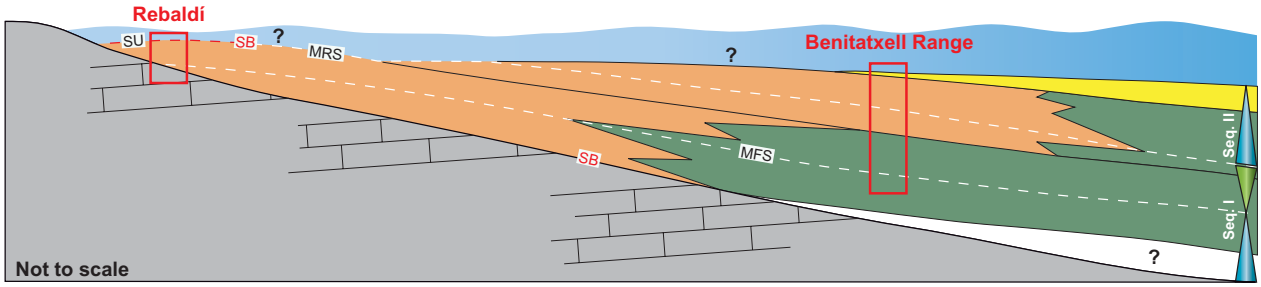

B Late regressive stage of Sequence I and early transgressive stage of Sequence II (latest Chattian)

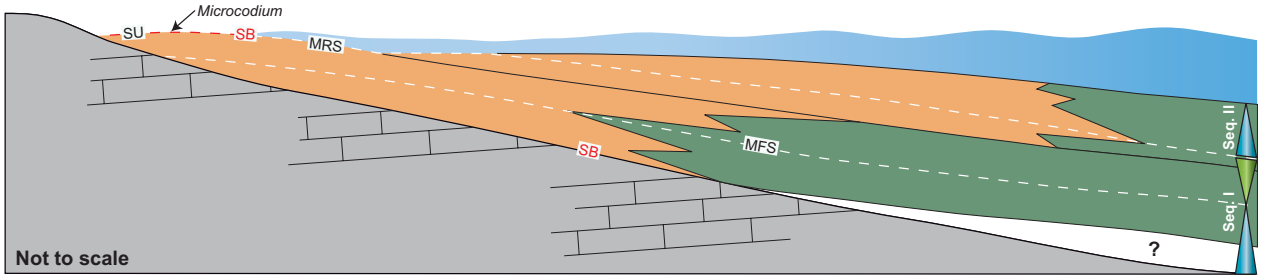

A Transgressive and early regressive stages of Sequence I (Rupelian?-late Chattian)